Identity of the shallowest acceptor in GaN

M. A. Reshchikov* **and D. O. Demchenko**

Department of Physics, Virginia Commonwealth University, Richmond, VA 23220, USA

B. McEwen and F. Shahedipour-Sandvik

College of Nanoscale Science and Engineering, SUNY-Albany, Albany, New York 12203, USA

Abstract

The Be-related ultraviolet luminescence (UVL_{Be}) band with a maximum at about 3.38 eV in GaN:Be is caused by the shallowest acceptor in GaN with the –/0 transition level at 0.113 eV above the valence band. The luminescent properties of this acceptor were studied in detail. First-principles calculations identify this acceptor as the $Be_{Ga}O_NBe_{Ga}$ complex. These calculations also predict a deep level, at 0.34 eV above the valence band. However, we were not able to find evidence for this level in photoluminescence experiments.

* E-mail: mreshchi@vcu.edu

I. INTRODUCTION

Wide-bandgap semiconductors, such as GaN and its alloys with AlN, attract significant attention from researchers due to their numerous applications in optical and high-power devices.[1-4] However, despite the impressive success of GaN-based technology, *p*-type doping remains a bottleneck because Mg, the only known viable acceptor in these semiconductors, is not shallow enough in GaN (the ionization energy is E_A = 0.22 eV), and it becomes too deep in AlGaN with increasing Al content (E_A = 0.5-0.6 eV in AlN). Alternative approaches, such as superlattice structures and polarization-induced hole doping, have been proposed.[5,6] However, these approaches have downsides, such as lower vertical than lateral conduction.[7,8] Co-doping of GaN and AlGaN with Mg and O also showed promising results with an apparent reduction of the E_A but limited progress was demonstrated.[9,10,11] Thus, there is a strong demand for a shallower acceptor in GaN, AlN, and AlGaN, i.e., which has a lower E_A than that of Mg. The Be_{Ga} acceptor was suggested as an alternative *p*-type dopant. There are several reports on conductive *p*-type GaN:Be,[12-16] and even *p*-type AlN:Be,[17-19] yet these materials are more often semi-insulating, and the reasons for inconsistent results remain unknown.

A shallow acceptor with E_A = 0.113 eV was experimentally found in GaN and initially (mistakenly) attributed to the isolated Be_{Ga} acceptor. This shallow acceptor is responsible for the photoluminescence (PL) band (called the UVL_{Be}) with the zero-phonon line (ZPL) at about 3.38 eV followed by LO phonon replicas.[20-23] However, recent PL studies provided convincing evidence that the Be_{Ga} is, in fact, a dual-nature acceptor[24] with two polaronic deep states at 0.38±0.03 eV and 0.33±0.05 eV above the valence band maximum (VBM) and a shallow state with a delocalized hole at 0.24±0.02 eV above the VBM at low temperatures.[25] The polaronic states are responsible for the broad yellow luminescence (YL_{Be}) band with a maximum at about

2.15 eV, whereas transitions via the shallow state can be observed only at $T > 100$ K as the ultraviolet luminescence band with the ZPL at ~3.26 eV (labeled UVL_{Be3}). Note that in recent first-principles calculations, where adjustments were made to reproduce the GaN bandgap, the polaronic states of the Be_{Ga} acceptor were predicted at 0.55-0.80 eV and no shallow states were reported.[26-29]

The findings of Ref. 25 indicated that the UVL_{Be} (3.38 eV) band cannot be caused by the isolated Be_{Ga} acceptor. Nevertheless, the defect responsible for the 3.38 eV band clearly contains Be and demonstrates features of the shallowest acceptor in GaN. Thus, identifying the 3.38 eV band in Be-doped GaN is not just an interesting puzzle; it could also lead to the discovery of new efficient *p*-type doping in III-nitride materials.

In this work, we present a comprehensive PL study of the UVL_{Be} (3.38 eV) band, which was detected in about fifty Be-doped GaN samples grown by metal-organic chemical vapor deposition (MOCVD) and molecular beam epitaxy (MBE) under various conditions. First-principles calculations attributed this PL band to the $Be_{Ga}O_NBe_{Ga}$ complex, which could be the shallowest acceptor in GaN with $E_A = 0.113$ eV.

II. METHODS

A. Samples

The UVL_{Be} (3.38 eV) band was studied in more than 50 GaN:Be samples grown by MOCVD and MBE. Several GaN:Be samples were selected for detailed analysis and illustrations (Table I). Samples with the prefix "R" are ~500 nm-thick GaN:Be layers grown by MOCVD on unintentionally doped GaN on c-plane sapphire substrates. Beryllium acetylacetonate ($Be(acac)_2$) from Strem Chemicals was used as a Be precursor. Nitrogen-rich conditions were maintained. Immediately after growth, the material was annealed *in situ* under flowing N_2 at 500 Torr and 750

°C for 30 min without removing from the growth chamber. The concentration of Be (Table I) was determined from secondary-ion mass-spectrometry (SIMS) measurements. The MOCVD samples were moderately contaminated with oxygen and magnesium impurities. The typical concentration of O from SIMS is 10^{17}-10^{18} cm^{-3}. The concentration of Mg_{Ga} acceptors could be estimated from PL measurements. For MOCVD samples, it varied in a wide range (between 10^{14} and 10^{16} cm^{-3}). The dislocation density was estimated to be lower than 10^{9} cm^{-2} from X-ray rocking curve scans. To study the effect of dislocations on PL spectra, several GaN:Be layers (not included in Table I) were grown on freestanding HVPE GaN substrates with a dislocation density of ~10^{6} cm^{-2}. We did not notice any significant difference in intensities of the YL_{Be} and UVL_{Be} bands in samples grown on sapphire and on freestanding GaN substrates and concluded that both PL bands are unrelated to dislocations. Samples 0408a and 0410a are Be-doped GaN layers grown by MBE at 675-770 °C on the c-plane sapphire substrate at West Virginia University.[30] The PL spectra from as-grown MBE GaN:Be samples often contain the GL2 and RL_{Be} bands attributed to the isolated V_N and the $Be_{Ga}V_N$ complexes, respectively. This confirms the assumption that the MBE GaN:Be samples were grown in Ga-rich conditions.[31] More details about GaN:Be samples grown by MBE can be found in Refs. 22 and 30. Selected samples were annealed in N_2 or N_2H_2 ambient for one hour at temperatures T_{ann} = 400-1000 °C.

Table I. Parameters of GaN:Be samples

Sample	Growth method	[Be] (cm^{-3})
R29	MOCVD	5×10^{18}
R41	MOCVD	2×10^{19}
R87	MOCVD	4×10^{18}
R96	MOCVD	3×10^{18}
0408a	MBE	5×10^{17}
0410a	MBE	1×10^{18}

B. Photoluminescence measurements

Steady-state PL (SSPL) was excited with a HeCd laser at 325 nm, dispersed by a 1200 rules/mm grating in a 0.3-m monochromator, and detected by a Peltier-cooled photomultiplier tube and a photon-counting module. Time-resolved PL (TRPL) was excited with a pulsed nitrogen laser and analyzed with an oscilloscope. A closed-cycle optical cryostat was used for temperatures between 18 and 320 K, and a high-temperature optical cryostat was used for temperatures between 100 and 680 K. The internal quantum efficiency for each PL band, η_i, was estimated by comparing the intensity after integrating over the PL band with that from calibrated GaN samples.[32-34] Other details of PL experiments can be found elsewhere.[32,35] The as-measured PL spectra were corrected for the measurement system's spectral response, and PL intensity was additionally multiplied by λ^3, where λ is the light wavelength, to present the PL spectra in units proportional to the number of emitted photons as a function of photon energy.[32,35]

C. Theory

Theoretical calculations were performed using the Heyd-Scuseria-Ernzerhof (HSE) hybrid functional[36] as implemented in the VASP code. The HSE functional was tuned to fulfill the generalized Koopmans' condition for the $Be_{Ga}O_NBe_{Ga}$ complex. Details of error corrections and Koopmans' tuning procedure for the deep and shallow states are described in Ref. 37. The resulting HSE parametrizations are obtained with values of the fraction of the exact exchange α of 0.245 and 0.33 for the deep and shallow states, respectively, of the $Be_{Ga}O_NBe_{Ga}$ complex (the range separation parameter is kept at 0.2 $Å^{-1}$). These parametrizations essentially eliminate the self-interaction energy from the defect state orbitals. However, they respectively underestimate and overestimate the HSE-calculated bandgap of the bulk GaN. Therefore, transition energies were calculated from the HSE defect total energies using the experimental bandgap of GaN $E_g^{exp} = 3.50$

eV. The –/0 thermodynamic transition level of the acceptor relative to the VBM (E_{VBM}) is calculated as $E(0/-) = E(-) - E_{VBM} - E(0)$, where $E(-)$ and $E(0)$ are the HSE total energies of the negative and neutral charge states of acceptor in their relaxed lattice geometries, respectively. The $E(-)$ and $E(0)$ total energies were corrected for the artificial interactions in periodic supercells, following the correction procedure in Ref. 37. The energy of the ZPL (E_0) is then $E_0 = E_g^{exp} - E(0/-)$, and that of the PL maximum is $\hbar\omega_{max} = E_0 - \Delta_{FC}$, where Δ_{FC} is the lattice relaxation energy following the transition at the PL maximum (Franck-Condon shift). All calculations were performed in 300-atom hexagonal supercells at the Γ-point, with plane-wave energy cutoffs of 500 eV. All defect atomic structures were relaxed using HSE to minimize the forces to 0.05 eV/Å or less. The configuration coordinate diagrams were obtained by performing parabolic fits into HSE computed transition energies (i.e., within the harmonic approximation) to map the atomic displacements ΔR_i onto the configuration coordinate Q following Ref. 38.

III. RESULTS

A. Experiment

1. Luminescence bands related to Be in GaN

Figure 1 shows PL spectra at 18 and 170 K from a representative GaN:Be sample grown by MBE and annealed at 850 °C. The UVL_{Be} band with the strongest peak at 3.362 eV (T = 18 K) is attributed to the ZPL of the Be-related shallow acceptor. It is followed by three phonon replicas separated by the energy of the LO phonon in GaN (91-92 meV). The YL_{Be} band is attributed to a deep polaronic state of the isolated Be_{Ga} acceptor. The near-band-edge (NBE) emission is dominated by the donor-bound exciton peak at 3.47 eV at T = 18 K.

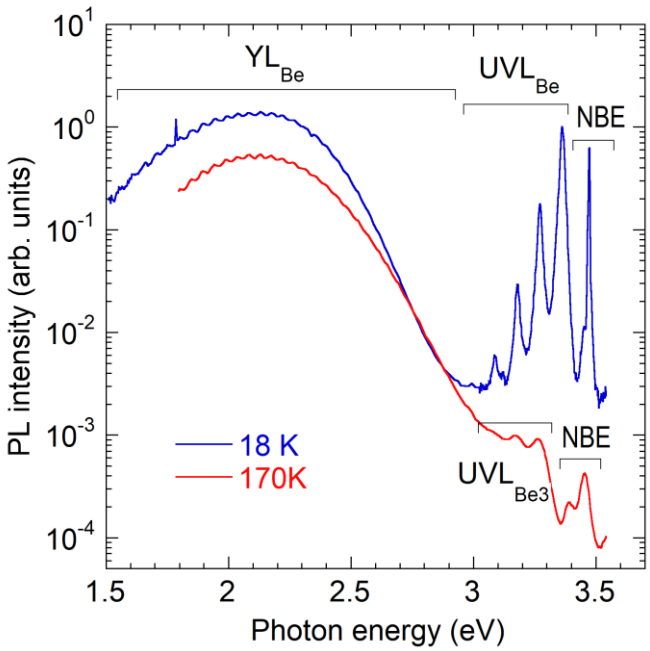

Fig. 1. SSPL spectra from Be-doped GaN grown by MBE (sample 0408a annealed for one hour in N_2 ambient at T_{ann} = 850 °C). P_{exc} = 0.02 W/cm^2.

With increasing temperature, the UVL_{Be} band quenches and disappears at $T \approx 120$ K. At higher temperatures, the isolated Be_{Ga} acceptor-related UVL_{Be3} band with a maximum at ~3.26 eV emerges (Fig. 1). The characteristic feature of the UVL_{Be3} and YL_{Be} bands is that their intensities ratio increases with temperature exponentially as

$$\frac{I_{Be3}^{UVL}}{I_{Be}^{YL}} = \delta \exp\left(-\frac{\Delta E}{kT}\right) \quad (1)$$

in all Be-doped GaN samples (about 50 samples grown by MOCVD and MBE for which the temperature dependence was studied).[25] Figure 2(a) shows this ratio for selected samples subjected to different experimental conditions. In all the cases (see more examples in Ref. 25), the UVL_{Be3} and YL_{Be} bands *correlate*, and the parameters of the fit vary in narrow ranges (ΔE = 140-150 meV and δ = 15-30). According to the model proposed in Ref. 25, ΔE is the distance between the deep

and shallow states of the Be_{Ga} acceptor ($\Delta E = E_{Be2} - E_{Be3}$), and δ is the ratio of PL lifetimes associated with these two states ($\delta = \tau_{Be2}/\tau_{Be3}$). This correlation of the UVL_{Be3} and YL_{Be} intensities is crucial evidence for the dual nature of the Be_{Ga} acceptor.[25] On the other hand, there is no correlation between the UVL_{Be} and YL_{Be} bands in the same samples (Fig. 2(b)). The temperature dependence of the UVL_{Be} and YL_{Be} intensities ratio in Fig. 2(b) is governed by the quenching of the UVL_{Be} band at $T > 60$ K. Moreover, the UVL_{Be} band was not observed in several samples, while the YL_{Be} band was always very strong. This indicates that the UVL_{Be} (3.38 eV) band is highly unlikely to be caused by the isolated Be_{Ga} acceptor. Below, the properties of the UVL_{Be} band, which is responsible for the shallowest acceptor in GaN, will be analyzed in detail.

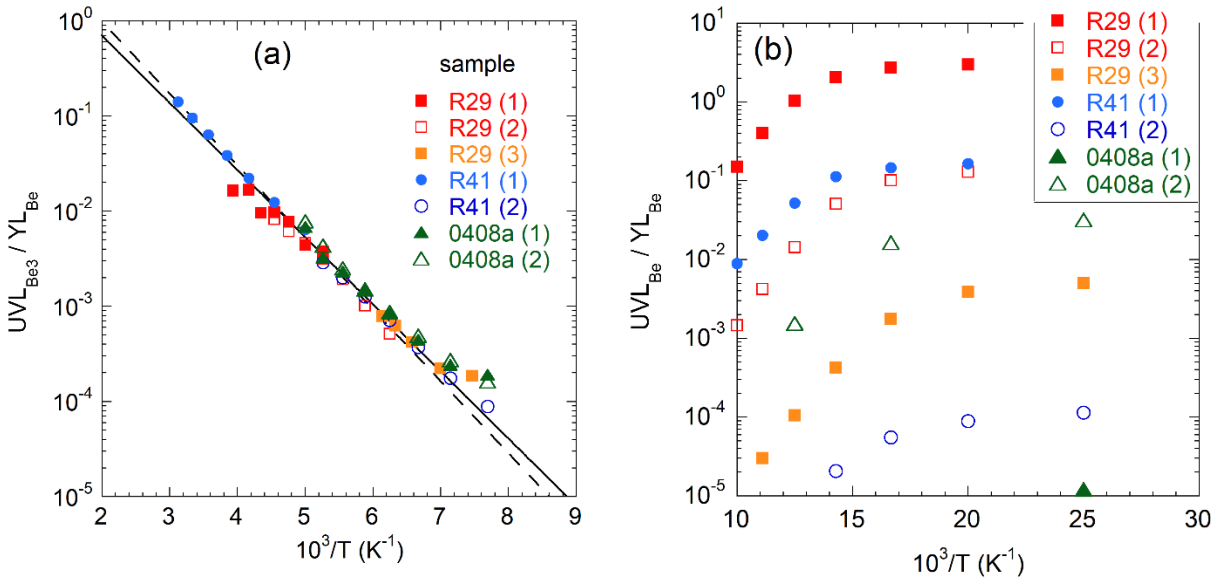

Fig. 2. Ratios of PL intensities as a function of inverse temperature. (a) UVL_{Be3}(3.26 eV)/YL_{Be}(2.15 eV) and (b) UVL_{Be}(3.38 eV)/YL_{Be}(2.15 eV). Experimental conditions: MOCVD GaN:Be sample R29 at P_{exc} = 50 W/cm^2 (1), 0.13 W/cm^2 (2), and 0.0001 W/cm^2 (3); MOCVD GaN:Be sample R41 at P_{exc} = 12 W/cm^2 (1) and 0.0001 W/cm^2 (2); MBE GaN:Be sample 0408a annealed at 550°C (1) and 900°C (2) and measured at P_{exc} = 0.02 W/cm^2. The lines in (a) are calculated using Eq. (1) with $\delta = 20$ and ΔE = 140 meV (the solid line) and $\delta = 32$ and ΔE = 150 meV (the dashed line).

2. Comparison of photoluminescence from Mg- and Be-related shallow acceptors

We established earlier that the UVL_{Be} band at $T = 18$ K is caused by a recombination of electrons at shallow donors with holes at a shallow acceptor with the level at 0.113±0.005eV,[23] the recombination process via the donor-acceptor pair (DAP) transition mechanism.[39] With increasing temperature, at $T \approx 50$ K, the DAP components are replaced with very similar components shifted by 20 meV to higher energy. They are attributed to transitions from the conduction band to the same acceptor, the eA transition mechanism. We observed such transformation of the UVL_{Be} band in all GaN:Be samples, including those grown by MBE,[23] MOCVD,[40] and in GaN grown by hydride vapor phase epitaxy (HVPE) and implanted with Be.[41]

The Huang-Rhys factor S for the UVL_{Be} band is defined as the ratio of intensities of the first phonon replica and the ZPL (about 0.2 in Fig. 1). The advantage of the studied MBE-grown GaN:Be samples is the absence of the Mg-related UVL_{Mg} band that may obscure the UVL_{Be} band spectrum at photon energies below 3.3 eV. On the other hand, our MOCVD-grown GaN:Be samples have better crystal quality, resulting in narrower PL lines. Unfortunately, Mg is a contaminant in our MOCVD growth, and the UVL_{Mg} band is commonly observed in the PL spectrum. Figure 3 compares the fine structure of PL in the UV region from two MOCVD-grown GaN:Be samples.

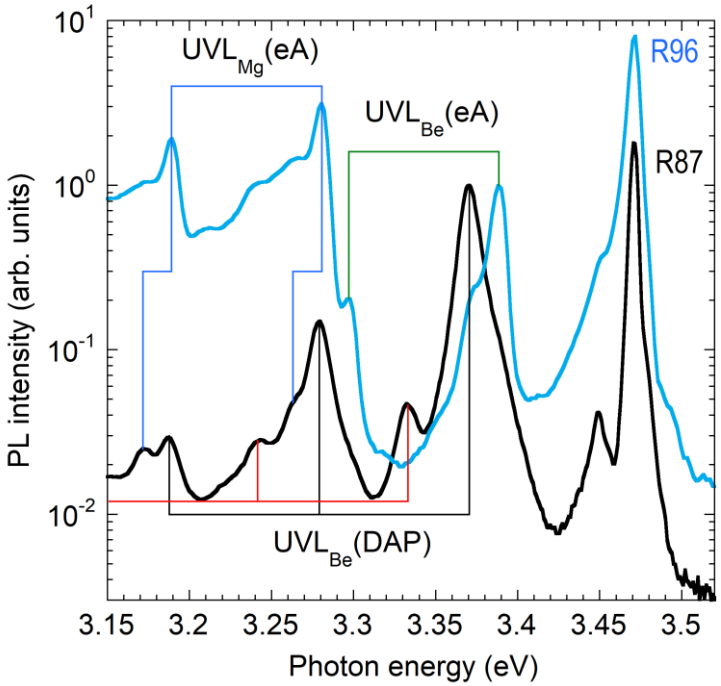

Figure 3. SSPL spectra (normalized at a maximum of the UVL_{Be} band) from two Be-doped GaN samples grown by MOCVD (R87 is as-grown GaN:Be and R96 is GaN:Be annealed at 1000 °C). T = 18 K and P_{exc} = 0.005 W/cm^2. The spectra are red-shifted by 8 meV to compensate for biaxial strain in GaN/sapphire layers.

For sample R87, S = 0.15, and the contribution of the UVL_{Mg} band is negligible at T = 18 K (it could be noticed at T = 100 K when the UVL_{Be} band is quenched). For sample R96, the UVL_{Mg} band is stronger than the UVL_{Be} band. Another distinction between the samples analyzed in Fig. 3 is that sample R96 was additionally annealed in N_2 ambient for one hour at T_{ann} = 1000 °C. The annealing led to a significant enhancement of eA components (relative to DAP components) in the UVL_{Mg} and UVL_{Be} bands. This effect was reproduced in all (total of four) MOCVD GaN:Be samples annealed at such high temperature and is attributed in the literature to a reduction of the shallow donor concentration.[42,43]

The PL spectra in Fig. 3 are red-shifted by 8 meV to compensate for the biaxial-strain-related blue shift of PL lines. Then, the DBE peak is at 3.471 eV, and its two-electron satellite is at 3.45

eV, which agrees with other reports for unstrained GaN.[44] The free exciton (FE) peak contributes as a high-energy shoulder to the DBE peak and can be better resolved at higher temperatures. The eA and DAP components of the UVL_{Be} band ZPL are at $\hbar\omega_{eA}$ = 3.3885 eV and $\hbar\omega_{DAP}$ = 3.3705 eV, respectively. They are followed by LO phonon replicas at distances multiple of 91.5 meV. For sample R87 (as well as for several other high-quality MOCVD GaN:Be samples), we also resolve phonon replicas shifted by $\hbar\Omega_0$ = 37.5 meV from the ZPL and its LO phonon replicas. We attribute these peaks to a pseudo-local phonon mode. The ZPL of the UVL_{Mg} band (the eA component in sample R96) is observed at $\hbar\omega_{eA}$ = 3.2805 eV.

The separation between the eA peaks of the UVL_{Be} and UVL_{Mg} bands is 108±1 meV, and their full width at half maximum (FWHM) is about 10 meV at T = 18 K. Observation of eA peaks at such low temperatures allows us to find more accurately the energy of the –/0 transition level above the VBM. Indeed, $E_A = E_g - \hbar\omega_{eA}$, where E_g is the GaN bandgap. By taking the following values for unstrained high-quality GaN, DBE at 3.471 eV, FE at 3.477 eV and E_g = 3.502 eV at T = 2 K,[45] we obtain E_A = 113.5 meV for the Be-related acceptor and E_A = 221.5 meV for the Mg_{Ga} acceptor.

The attribution of the UVL_{Be} and UVL_{Mg} peaks to eA and DAP transitions has been verified by careful analysis of their evolution with variations in temperature or excitation intensity P_{exc}. Figure 4 shows how the DAP component of the UVL_{Be} ZPL shifts with increasing excitation intensity. The shift is identical to that of the UVL_{Mg} ZPL in high-quality undoped GaN grown by HVPE (shown with empty symbols in Fig. 4).

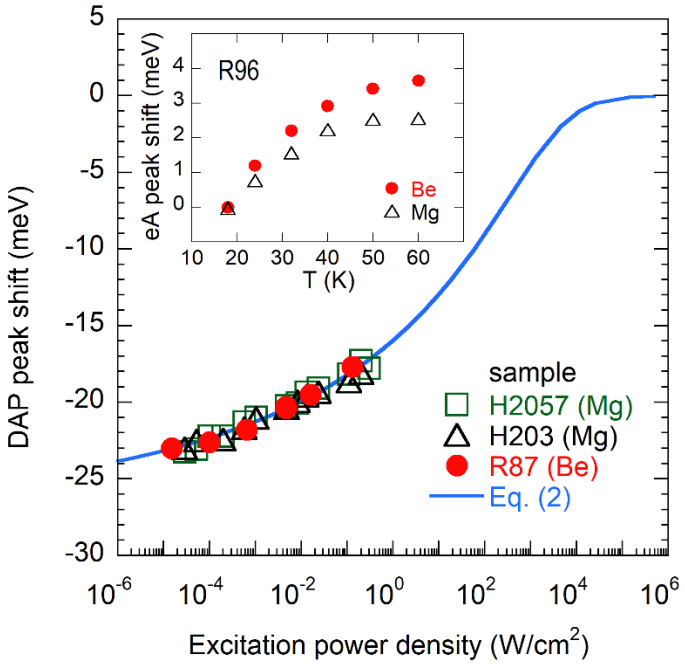

Figure 4. The shift of the DAP component of the UVL band ZPL (for Be in GaN:Be and for Mg in undoped GaN) with excitation intensity at $T = 18$ K. The inset shows the shift of the eA component of the UVL band ZPL in GaN:Be sample R96 with increasing temperature. The line is calculated using Eq. (2).

The shift of the DAP component of ZPLs (by about 7 meV with increasing P_{exc} from 10^{-5} to 0.3 W/cm^2) is very similar for several acceptors in GaN,[32,46] because the same shallow donor (O_N with the ionization energy of E_D = 33 meV)[47] is unintentionally introduced with typical concentrations in the 10^{17}-10^{18} cm^{-3} range. The average separation of distant pairs can be estimated as $R_m = (2\pi N_D)^{-1/3}$, where N_D is the concentration of shallow donors.[39] The value $\hbar\omega_{eA} - \hbar\omega_{DAP} \approx$ 20 meV, which is smaller than E_D by the Coulomb interaction energy (~13 meV), implies that $R_m \approx$ 12 nm and $N_D \approx 10^{17}$ cm^{-3} for samples R87 and R96 analyzed above.

The dependence of $\hbar\omega_{DAP}$ on P_{exc} can be found from the following expression [48]

$$P_{exc} = D\frac{E_C^{\,3}}{E_B - E_C}\exp\left(-\frac{4E_B}{E_C}\right), \quad (2)$$

where D is a constant, $E_C = \hbar\omega_{DAP} - (E_g - E_D - E_A)$, and $E_B = \kappa/R_B$ is the Coulomb interaction energy for a pair with a separation equal to the Bohr radius R_B of a shallower component in the effective-mass approximation. The total shift of the DAP-related PL band in a wide range of P_{exc} is not expected to exceed the ionization energy of the shallower component.[48]

The TRPL experiments also confirmed the DAP nature of the UVL_{Be} band at $T = 18$ K. The PL decay after a laser pulse is nonexponential, $I^{PL}(t) \propto t^{-n}$ with $n \approx 1$. The peak maximum gradually redshifts with time delay, totally by 7 meV between 0.3 and 100 μs. Such behavior is typical for DAP transitions in GaN and other semiconductors.[49,50]

With increasing temperature from 18 to 60 K, both the DAP and eA components of the UVL_{Be} and UVL_{Mg} bands shift to higher photon energy by about 3 meV. The inset in Fig. 4 shows the $\hbar\omega_{eA}(T)$ dependences for sample R96, in which the eA components are well resolved in a wide range of temperatures. Similar shifts were observed earlier for the UVL_{Be} and UVL_{Mg} bands with increasing temperature from 4 to 50 K in a bulk GaN:Be sample grown by the high nitrogen pressure method.[51] From the above analysis, we conclude that the UVL_{Mg} and UVL_{Be} bands are caused by two shallow acceptors in GaN: the Mg_{Ga} and a Be-related acceptor other than the isolated Be_{Ga}.

3. Arguments favoring the shallowest acceptor attribution

The fact that a PL line is found at 0.113 eV below the E_g does not necessarily mean that it is caused by an acceptor with the –/0 level at 0.113 eV above the VBM (which would be the shallowest

acceptor in GaN to date) because the attribution of PL lines is not always straightforward. Below, we will consider alternative attributions and provide arguments in favor of the shallowest acceptor.

Small Huang-Rhys factor. In general, with increasing ionization energy of an acceptor, E_A, a bound hole becomes more localized. This results in increasing electron-phonon coupling, the strength of which is measured with the Huang-Rhys parameter S.[52,53] This parameter can be found from the PL band's shape for broad, structureless PL bands (Sec. IIIA6) or as a ratio of intensities of the first phonon replica and the ZPL peak when the phonon-related fine structure can be resolved.[32,54] Figure 5 shows the values of S for the UVL_{Be} and UVL_{Mg} bands in comparison with the experimentally found S values for other known acceptors and donors in GaN.[32] Thus, the shape of the UVL_{Be} band corresponds to a very shallow acceptor, shallower than Mg_{Ga}.

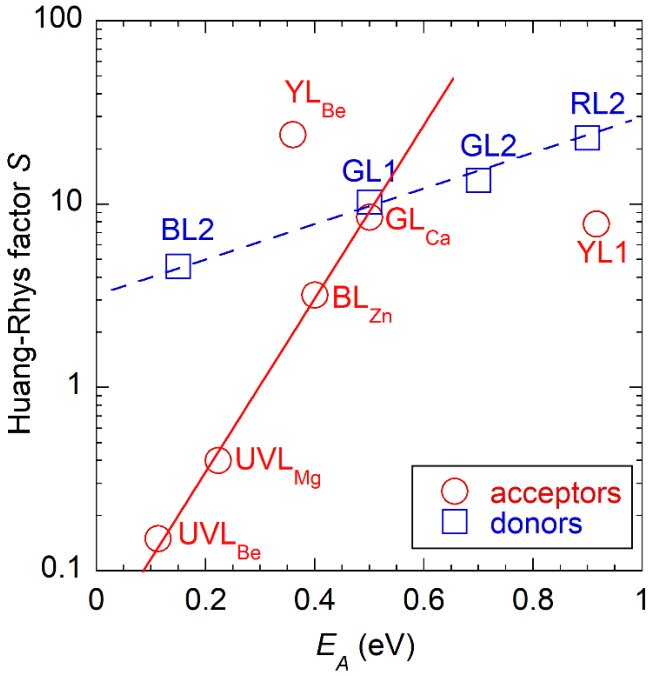

Figure 5. Dependence of the Huang-Rhys factor on ionization energy for acceptors and donors in GaN. Lines are guides to the eye.

DAP mechanism transforms into eA mechanism. PL spectra from several acceptors in GaN reveal the ZPL and phonon-related fine structure. In addition to Mg_{Ga}, these are Zn_{Ga} (the BL_{Zn} band with a maximum at 2.9 eV), C_N (the YL1 band with a maximum at 2.17 eV), and a Fe-related RY3 defect (the YL3 band with a maximum at 2.07 eV).[32] For all these acceptors, the DAP peaks are observed at $T < 20$ K, and the eA peaks emerge at $T > 40$ K. Exactly the same transformation of PL was observed for the UVL_{Be} band in all GaN:Be samples (except for the samples annealed at 1000 °C where the eA peaks were observed already at 18 K). Such behavior is different from that for PL bands caused by donors in GaN where the PL is always caused by internal transitions: from an excited state near the conduction band to the ground state of the same defect.[32] For the donors, the ZPL does not shift with a variation of excitation intensity, and the PL decay is exponential even at very low temperatures.

Large hole- and electron-capture coefficients. One distinction of the UVL_{Be} band from other acceptor-related PL bands in GaN is that the UVL_{Be} band is very weak (if present at all) in conductive *n*-type GaN:Be. Indeed, other acceptors (often caused by unintentional contamination with impurities, such as Mg, Zn, and C) are efficient centers of radiative recombination in *n*-type GaN because they capture holes very quickly due to the attractive nature of negatively charged acceptors. In such samples, it is easy to experimentally find important characteristics and parameters of defects, including their concentration, hole-capture, and electron-capture coefficients.[32] Be is not a common contaminant in GaN growth. When it is intentionally introduced during growth or by ion implantation, the samples are usually semi-insulating with an unknown conductivity type. However, in some GaN:Be samples the concentration of shallow O_N donors exceeds the concentration of acceptors, and such samples are conductive *n*-type. We have discovered only three such samples grown by MOCVD (out of more than 50) and one *n*-type

sample grown by MBE (out of 20). No UVL_{Be} band could be found in these four samples (it could be in part because of strong excitonic emission and LO phonon replicas of the NBE peaks near 3.38 eV in *n*-type samples). More conductive *n*-type samples were also obtained after co-implantation of Si-doped GaN with Be and F ions, and three Si-GaN:Be,F samples revealed the UVL_{Be} band.[41] From the analysis of SSPL and TRPL at different temperatures in these samples we determined electron- and hole-carrier capture coefficients for the UVL_{Be}-related defect: C_n = 1×10^{-11} cm^3/s and C_p = $(1\text{-}20)\times10^{-7}$ cm^3/s, respectively. While there is significant uncertainty in the value of C_p, the extremely large value of C_n supports the attribution of the UVL_{Be} band to the shallowest acceptor and matches the trend for other acceptors in GaN (Fig. 6). Note that the C_n could not be found for donors in GaN because the eA emission is not observed. As for the weakness (or absence) of the UVL_{Be} band in conductive *n*-type GaN:Be, we conclude that the related acceptors are unlikely to form in such samples due to unfavorable growth conditions. We will return to this issue in Sec. IV.

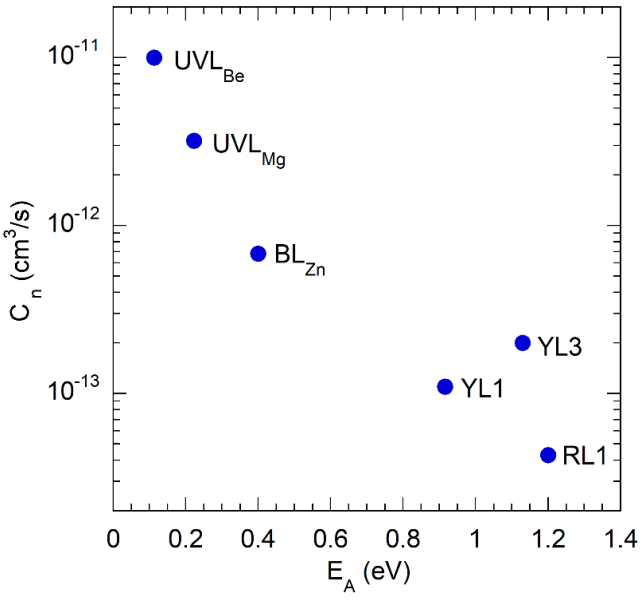

Fig. 6. The electron-capture coefficient for acceptors in GaN obtained from TRPL experiments.

4. Thermal quenching of the UVL_{Be} band

Figures 7 and 8 show an example of PL spectrum evolution with increasing temperature from 18 to 100 K and the Arrhenius plot for the UVL_{Be} intensity at selected P_{exc}. The UVL_{Be} band in semi-insulating GaN:Be is quenched with increasing temperature above ~70 K by the tunable quenching mechanism.[34] This quenching mechanism is common for PL from semi-insulating GaN and other semiconductors.[55] Defect-related PL intensity in such samples drops above a critical temperature T_0. The main feature of this mechanism is that T_0 increases with increasing P_{exc}. At low temperatures ($T < T_0$), an inverse population of charge carriers occurs in conditions of SSPL. Namely, dominant nonradiative donors become saturated with photogenerated electrons (because they capture nonequilibrium electrons quickly), while acceptors become saturated with holes (because of the fast capture of holes by acceptors). The drop of PL at T_0 is explained by the thermal emission of holes from the acceptors to the valence band, which initiates a transformation of the charge carrier population from inverse to equilibrium.

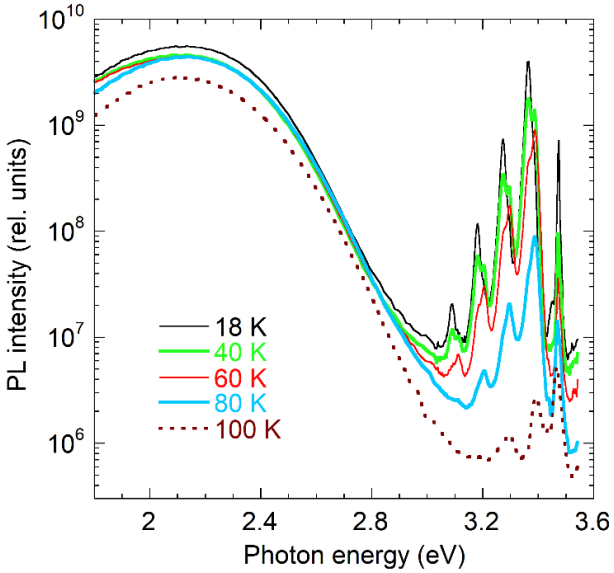

Figure 7. Evolution with temperature of PL spectrum in GaN:Be (MBE GaN:Be sample 0408a annealed at T_{ann} = 850 °C). P_{exc} = 0.005 W/cm^2.

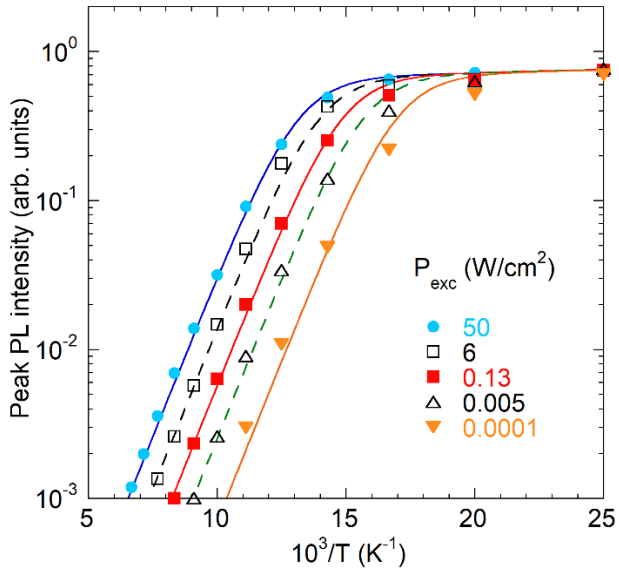

Figure 8. Temperature dependence of the UVL_{Be} intensity (normalized at T = 18 K) for MOCVD GaN:Be sample R29 at selected P_{exc}. The lines are calculated using Eq. (3) with E_A = 85 meV and the following parameter C: 4×10^5 (P_{exc} = 50 W/cm^2), 9×10^5 (6 W/cm^2), 2.2×10^6 (0.13 W/cm^2), 5×10^6 (P_{exc} = 0.005 W/cm^2), 1.8×10^7 (0.0001 W/cm^2).

In the case of the UVL_{Be} band, the quenching is tunable but not abrupt. Such dependence is expected when a shallow acceptor is quenched first, but the transformation of the charge carrier population from inverse to equilibrium occurs at higher temperatures – when a deeper acceptor with higher concentration is quenched.[56] Such behavior, called the two-step quenching, was observed in semi-insulating GaN samples doped with Zn and contaminated with Mg.[56] The quenching of the Mg-related UVL_{Mg} band at T > 100 K was tunable by P_{exc} but not abrupt, and only the second step of the PL quenching associated with the Zn-related BL_{Zn} band was abrupt and tunable. According to the two-step quenching mechanism, the quenching of the shallow acceptor occurs with the activation energy E_A equal to the acceptor ionization energy.

The $I^{PL}(T)$ dependence (Fig. 8) can be formally described with the following expression

$$I^{PL}(T) = \frac{I^{PL}(0)}{1 + C\exp\left(\frac{-E_A}{kT}\right)}, \quad (3)$$

where parameter C decreases with increasing P_{exc}.[56] The slope of the UVL_{Be} quenching reveals E_A = 60-95 meV in different samples (85 meV in Fig. 8). Note that the value of E_A from the Arrhenius plot is typically smaller than E_A found from PL spectroscopy at low temperatures (often by ~30 meV) due to potential fluctuations, variation in E_A with temperature, nonexponential PL decay, and other reasons.[55-57] Thus, the E_A from the Arrhenius plot agrees well with E_A = 113 meV obtained from low-temperature PL spectroscopy.

In summary, all experimental data indicate that the UVL_{Be} band is caused by electron transitions from shallow donors (at $T < 50$ K) or predominantly from the conduction band (at $T > 50$ K) to a shallow acceptor with the –/0 transition level at 0.113 eV above the VBM. Deep donors in GaN sometimes have levels close to the valence band (such as the C_NH_i complex with E_A = 0.15 eV above the VBM, the donor responsible for the BL2 band with a maximum at 3.0 eV).[58] However, the electron-phonon coupling is strong for such defects (large S), and PL is caused by internal transitions – from an excited state near the conduction band to the ground state. The UVL_{Be} band also cannot be attributed to electron transitions from an unknown donor to the valence band. Such transitions are not observed in GaN (mostly because of the lack of samples with reasonably high concentrations of free holes at cryogenic temperatures).[32] Finally, it is unlikely that the UVL_{Be} band has an excitonic nature. Excitons bound to structural defects or point defects gettered by extended defects can cause sharp PL lines at photon energies between 2.7 and 3.45 eV (the so-called Y lines).[59] However, the temperature behavior of the UVL_{Be} band (the transformation from the DAP to eA type transitions) and TRPL features (nonexponential and relatively slow decay of

PL at low temperature and exponential decay at $T = 50$ K with $\tau_0 = 0.3$ μs in a conductive *n*-type sample) are inconsistent with the excitonic nature.

5. Effect of annealing

Previously, the effect of thermal annealing on the UVL_{Be} band was studied only for MBE-grown GaN doped with Be. For MBE GaN:Be samples grown at UWV, annealing during two hours in N_2 ambient at $T_{ann} = 900$ °C consistently resulted in the appearance or significant enhancement of the UVL_{Be} band.[22,30,60] Interestingly, others reported on strong UVL_{Be} band in GaN:Be samples grown by MBE at 740-750 °C without mentioning post-growth annealing.[20,21,61] We investigated the effect of annealing at different temperatures on the intensity of the UVL_{Be} band in Be-doped GaN samples grown by MBE (from UWV) and MOCVD (from SUNY).

In as-grown MBE GaN:Be samples, the UVL_{Be} band was either very weak or absent. It emerges at $T_{ann} > 700$ °C and its intensity increases by orders of magnitude in a narrow temperature range (Figs. 9 and 10). The intensities of the YL_{Be} and NBE bands remained nearly unchanged in this temperature range. This indicates that the Be-containing shallow acceptor responsible for the UVL_{Be} band is passivated in MBE-grown GaN:Be, and it can be activated by the annealing. The annealing temperature of 700-800 °C corresponds to an activation energy of about 3.0 eV. It is likely that either H_i or V_N donors (which are both mobile at growth temperatures) passivate the Be-containing shallow acceptor. However, additional annealing in H_2 ambient at $T_{ann} = 550$ °C or in N_2+H_2 ambient at T_{ann} = 600-850 °C did not cause any significant changes in the UVL_{Be} intensity. This result contrasts with findings for the C_N acceptor in GaN, which could be reversibly passivated with hydrogen by annealing in N_2+H_2 ambient and activated by annealing in N_2 ambient.[58]

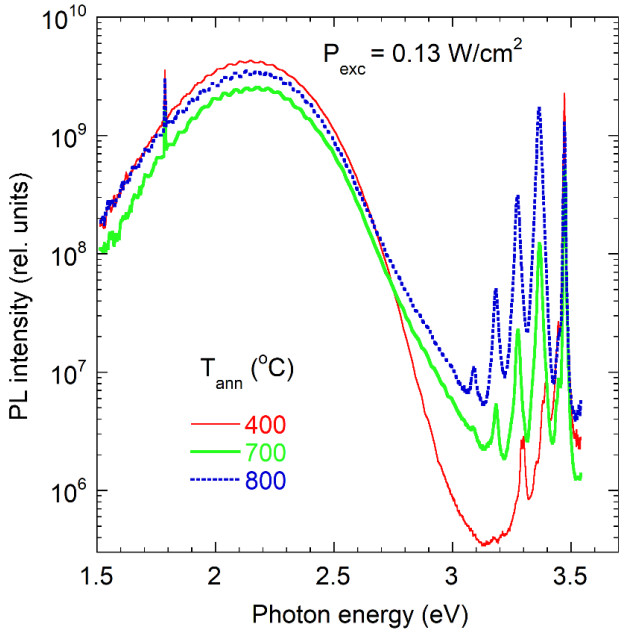

Fig. 9. The PL spectra at T = 18 K from MBE-grown GaN:Be (sample 0408a) annealed at selected temperatures in N_2 for one hour. For T_{ann} = 400 °C, the PL spectrum at $\hbar\omega$ = 3.2-3.4 eV reveals LO phonon replicas of excitonic lines and no traces of the UVL_{Be} band.

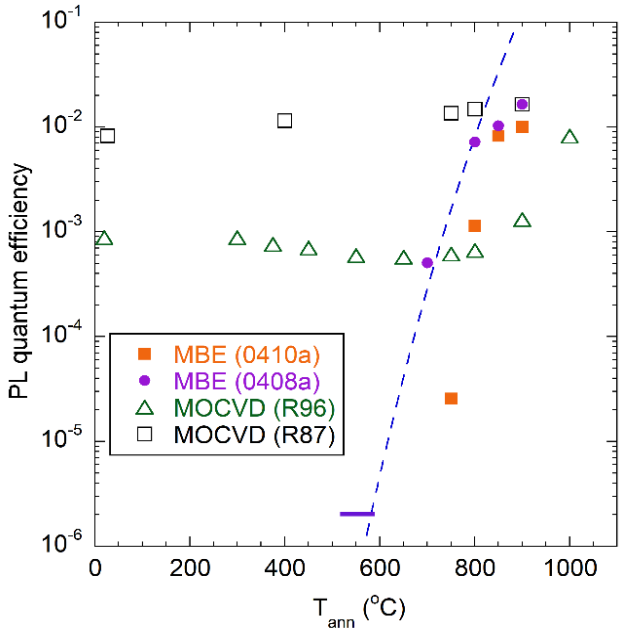

Fig. 10. PL quantum efficiency of the UVL_{Be} band in two MBE and two MOCVD GaN:Be samples as a function of annealing temperature. The horizontal bar at T_{ann} = 550 °C indicates that the UVL_{Be} efficiency for sample 0408a was lower than 2×10^{-6} – the background level. The dashed line is calculated dependence $10^{12}\exp(-E_a/kT)$ with E_a = 3 eV.

Most of our GaN:Be samples grown by MOCVD were annealed immediately after growth in flowing N_2 at 750 °C for 30 min without removing from the growth chamber. However, three samples were grown without any annealing. We did not notice any significant difference between PL spectra from annealed and not annealed samples. Additionally, selected MOCVD samples were annealed for one hour in N_2 at different temperatures. In samples where the UVL_{Be} band was strong after the growth, its variation with T_{ann} was insignificant (sample R87 in Fig. 10). In some as-grown MOCVD GaN:Be samples the UVL_{Be} band was weak or could not be resolved because its position was close to the LO replica of the DBE line. In such samples, the UVL_{Be} intensity increased with T_{ann} but much slower than in MBE GaN:Be samples (sample R96 in Fig. 10). The effect of annealing on GaN:Be samples grown by MBE and MOCVD will be discussed in more detail in Sec. IV.

6. Search for a deep polaron state

Some acceptors are predicted to have a dual nature (a shallow state with a delocalized hole and a deep state with a localized hole).[24] Experimentally, the dual nature was convincingly confirmed only in one case – for the Be_{Ga} acceptor in GaN.[25] Normally, one would expect that holes are localized at the deeper state at low temperatures. PL from the shallow state may appear with increasing temperature due to the Boltzmann distribution of holes between the deep and shallow states. Such interplay between PL from deep and shallow states of the same acceptor (identical in different samples) was observed for the Be_{Ga} acceptor in GaN.[25] PL from the shallow state can be observed at low temperatures only if a significant potential barrier exists between the two states. In this case, with increasing temperature, PL from the shallow state is expected to be replaced by PL from the deep state after the system overcomes the potential barrier (this will be discussed in more detail in Sec. IIIB2).[25] Below, we will report on the search for the deep state

that could be associated with the UVL_{Be}-related acceptor performed by varying experimental conditions.

In several GaN:Be samples (both MOCVD- and MBE-grown) the saturation of the YL_{Be} band was accompanied by the emergence of a blue luminescence band (labeled BL_{Be}) with a maximum at 2.6 eV (Fig. 11). For MOCVD GaN:Be sample R87, the NBE intensity increased superlinearly with P_{exc} (what is typical for semi-insulating GaN), and the UVL_{Be} intensity increased linearly between 0.0001 and 0.13 W/cm^2. The saturation of the YL_{Be} band began at about 0.005 W/cm^2. At higher P_{exc}, a shoulder appeared at its high-energy side (BL_{Be} in Fig. 11).

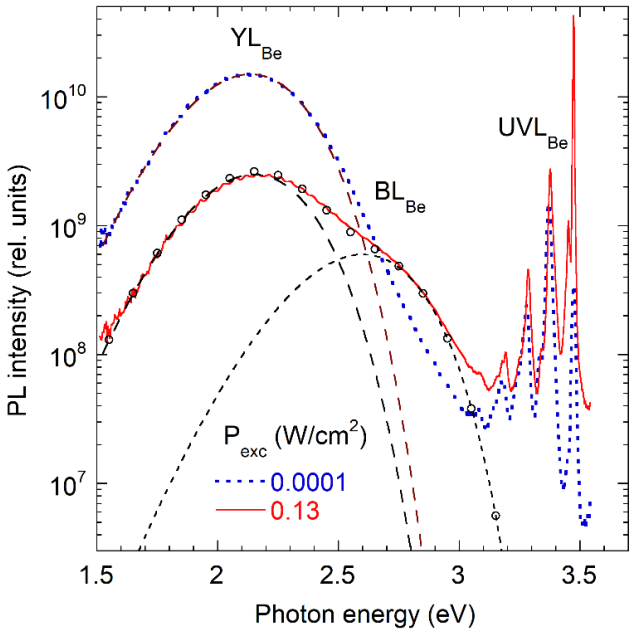

Fig. 11. Low-temperature (18 K) PL spectra from MOCVD GaN (sample R87) at two P_{exc} divided by the excitation intensity. The BL_{Be} band emerges with increasing P_{exc}. The dashed lines are calculated using Eq. (4) with the following parameters: S_e = 23, E_0^* = 3.2 eV, $\hbar\omega_{max}$ = 2.15 eV (the YL_{Be} band); S_e = 12, E_0^* = 3.4 eV, $\hbar\omega_{max}$ = 2.6 eV (the BL_{Be} band). Δ = 0 for P_{exc} = 0.13 W/cm^2 and Δ = -15 meV for P_{exc} = 0.0001 W/cm^2. Empty circles show the sum of the calculated YL_{Be} and BL_{Be} shapes at P_{exc} = 0.13 W/cm^2.

To deconvolute the PL spectra, the shapes of broad PL bands were simulated with the following expression obtained in a one-dimensional configuration coordinate model [62]

$$I^{PL}(\hbar \qquad \hbar \qquad \left[-2S_e \left(\sqrt{\frac{E_0^* - \hbar}{d_{FC}^g}} \qquad 1 \right)^2 \right]. \tag{4}$$

Here, S_e is the Huang-Rhys factor in the excited state of the defect, $d_{FC}^g = E_0^* - \hbar\omega_{max}$ is the Franck-Condon shift in the ground state, $E_0^* = E_0 + 0.5\ \hbar\Omega_e$, E_0 is the ZPL energy, $\hbar\Omega_e$ is the energy of the effective phonon mode in the excited state, $\hbar\omega$ and $\hbar\omega_{max}$ are the photon energy and position of the PL band maximum, respectively. The Δ is a small shift of the PL band maximum (< 0.02 eV) due to several reasons, such as the DAP/eA nature of transition, the presence of local electric fields, and in-plane biaxial strain in thin GaN layers grown on sapphire substrates. The parameters for the YL_{Be} band have been previously found from the analysis of the band shape in many GaN:Be samples grown by MBE and MOCVD (S_e is slightly decreased here to account for a small broadening of the band).[25,32,63] The shape and position of the BL_{Be} band were reconstructed from the analysis of PL from more than ten GaN:Be samples measured at high P_{exc}. Figure 12 shows the PL spectra from GaN:Be sample with the strongest contribution of the UVL_{Be} band measured at high P_{exc} and selected temperatures. The PL spectra were deconvoluted by using shapes of the YL_{Be} and BL_{Be} bands, and the integrated PL intensities were converted to PL quantum efficiencies (Fig. 13). The quenching of the UVL_{Be} and BL_{Be} bands begins at ~70 and 100 K, with E_A = 85 and 120 meV, respectively.

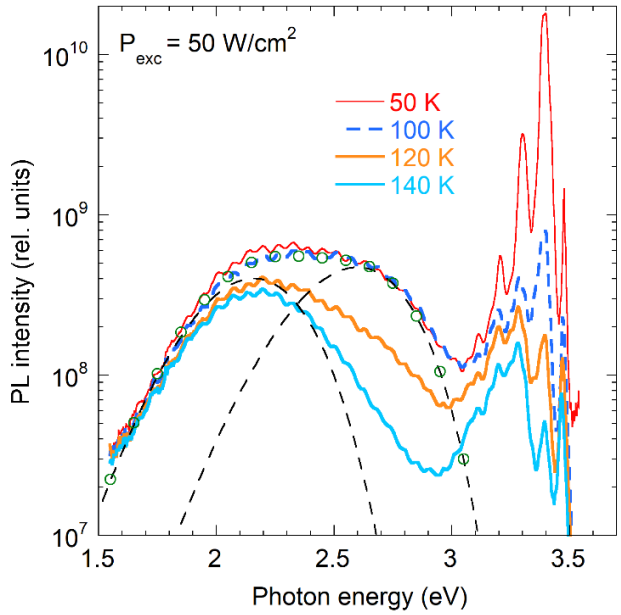

Fig. 12. Evolution of PL spectrum with temperature for MOCVD GaN:Be sample R29. The dashed lines show the shapes of the YL_{Be} and BL_{Be} bands at $T = 100$ K calculated by using Eq. (4) with the following parameters: $S_e = 24$, $E_0^* = 3.2$ eV, and $\hbar\omega_{max} = 2.15$ eV for the YL_{Be} band and $S_e = 12$, $E_0^* = 3.4$ eV, and $\hbar\omega_{max} = 2.6$ eV for the BL_{Be} band.

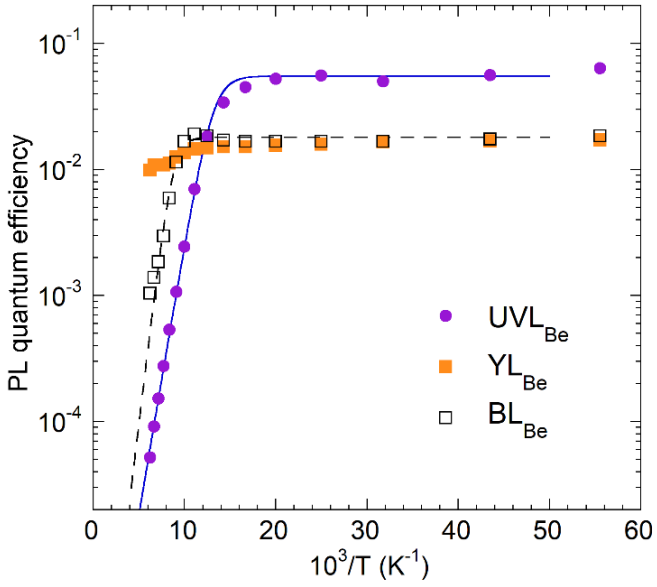

Fig. 13. Temperature dependence of PL quantum efficiencies for three PL bands in GaN:Be sample R29. The lines are calculated using Eq. (3) with the following parameters: $\eta_0 = 0.055$, $C = 2\times10^5$ and $E_A = 85$ meV (the solid line), and $\eta_0 = 0.018$, $C = 2\times10^5$ and $E_A = 120$ meV (the dashed line).

An important feature of the BL_{Be} band is exponential decay after a laser pulse at 18 K, the lowest temperature accessible in our experiment. The BL_{Be} band lifetime, τ, is 0.75±0.15 μs and sample-independent (in six samples where TRPL of the BL_{Be} band was studied). Such behavior is typical for internal transitions from a shallow excited state near the conduction band to the ground state of a donor in GaN.[32] This PL band could be caused by transitions via the 0/+ level of the Be_{Ga} defect located at 0.12-0.15 eV above the VBM. More statistical data are needed to establish the correlation between the YL_{Be} and BL_{Be} bands before they can be reliably attributed to two charge states of the Be_{Ga}. For the current work, it is important that there is no clear correlation between the BL_{Be} and UVL_{Be} bands. At least, we can find several samples revealing the UVL_{Be} band and no BL_{Be} band. This indicates that the BL_{Be} band is unlikely to be caused by transitions via a deep state of a dual-nature acceptor with the shallow state responsible for the UVL_{Be} band at 3.38 eV. The suspected deep state of the UVL_{Be}-related acceptor may still hide under the YL_{Be} and BL_{Be} bands but then its intensity must be very weak.

B. Theory

1. First-principles calculations

Since the experiment strongly suggests that the UVL_{Be} band originates from a Be-related shallow acceptor, other than the isolated Be_{Ga}, we have performed the initial preliminary search for a Be-related acceptor, with the results published in Ref. 63. In that work, we have calculated isolated Be defects in GaN (Be_{Ga}, Be_N, and Be_i) along with the complexes among them and with common native defects (V_N, V_{Ga}, N_i) and oxygen donor (O_N). Of the defects analyzed in the reference above, only the isolated Be_{Ga} and $Be_{Ga}O_NBe_{Ga}$ exhibited shallow acceptor transition levels. However, the latter was dismissed for having a low binding energy (we address this below). The only other defect that exhibited acceptor properties for the Fermi level around midgap was the $Be_{Ga}V_NBe_{Ga}$

complex, which was initially used in an attempt to explain the Be-related yellow YL_{Be} band. We later revised the attribution of the YL_{Be} band to the deep polaronic transition level of the isolated Be_{Ga} acceptor.[25] The above reference also provides convincing evidence that the UVL_{Be} band at 3.38 eV did not originate from the shallow state of the same Be_{Ga} acceptor. Therefore, since the $Be_{Ga}O_NBe_{Ga}$ is the only other Be-related shallow acceptor we find, here we revisit this defect complex in order to analyze its possible relation to the shallow UVL_{Be} band.

Koopmans tuned HSE calculations predict the co-existence of both deep polaronic and shallow states of the $Be_{Ga}O_NBe_{Ga}$ acceptor (Fig. 14), somewhat similar to the case of the isolated Be_{Ga} acceptor. There are two deep polaronic states of the neutral $Be_{Ga}O_NBe_{Ga}$ acceptor, with the hole localized on the nitrogen atom nearest to Be_{Ga} along the wurtzite *c*-axis (Fig. 14(a)), and the hole localized along one of the three in-plane Be-N bonds (Fig. 14(b)). There is also a shallow state of the neutral $Be_{Ga}O_NBe_{Ga}$ acceptor, which, in contrast to the isolated Be_{Ga}, is significantly more delocalized (Fig. 14(c)).

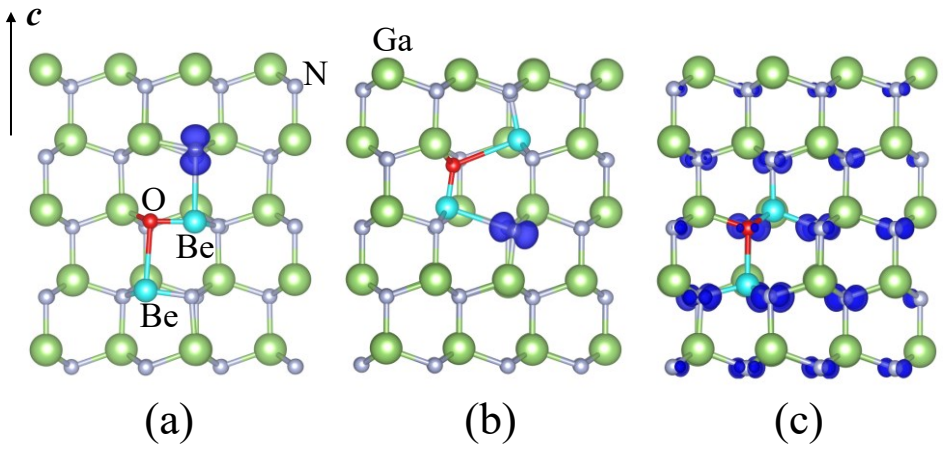

Fig. 14. Isosurfaces of the spin density of the hole localized on the neutral $Be_{Ga}O_NBe_{Ga}$ acceptor at 10% of the maximum value. (a) The deep polaronic state localized along the wurtzite *c*-axis; (b) in-plane deep polaronic state; (c) shallow state.

The $Be_{Ga}O_NBe_{Ga}$ acceptor complex consists of the tightly bound $Be_{Ga}O_N$ dimer, with a Be-O bond of 1.6 Å, and the second Be_{Ga} that is weaker bound with a Be-O bond length of 2.6 Å. The structure of the $Be_{Ga}O_NBe_{Ga}$ acceptor in the deep small polaronic states (Fig. 14 (a,b)) is characterized by significant lattice distortions. In these states, the hole is localized on the nitrogen atom that is the nearest neighbor of Be_{Ga}, where the Be-N bond is increased to 2.7 Å, in comparison with the 1.96 Å Ga-N bond. The total energies of the two configurations of the small polaron are very close, with the in-plane polaron having a total energy of 0.03 eV lower than that of the *c*-axis polaron. The polaronic lattice distortions are slightly larger than those in the isolated Be_{Ga} acceptor, where the Be-N bond was calculated to be 2.6 Å.[25]

The shallow state of $Be_{Ga}O_NBe_{Ga}$ acceptor is much more symmetric, with all Be-N bonds equal to 1.8 Å, and two slightly different Be-O bonds of 2.0 and 2.1 Å. The hole in this state is very weakly localized around the $Be_{Ga}O_NBe_{Ga}$ acceptor and is not fully reproduced in a 300-atom supercell.

The binding energy of the $Be_{Ga}O_NBe_{Ga}$ acceptor with respect to separation into a $Be_{Ga}O_N$ and Be_{Ga} is a relatively low 0.3 eV and practically independent of the Fermi energy. This binding energy is defined as the formation energy difference between the isolated constituents ($Be_{Ga}O_N$ plus Be_{Ga}) and the $Be_{Ga}O_NBe_{Ga}$ complex. The binding energy of 0.3 eV does not necessarily imply that $Be_{Ga}O_NBe_{Ga}$ complex is unstable. HSE tests using *ab initio* molecular dynamics on the GaN surface suggest that on the surface $Be_{Ga}O_NBe_{Ga}$ defect is stable at the MOCVD growth temperatures. (Note, we did not perform detailed *ab initio* molecular dynamics modeling of MOCVD growth, which is beyond the scope of this work.) Once formed during sample growth, this complex requires large energies to dissociate in the bulk GaN. Namely, our HSE calculations show that moving the Be atom from the Ga site of the $Be_{Ga}O_NBe_{Ga}$ complex into the nearby

interstitial (Be_i), which leaves behind a gallium vacancy V_{Ga}, leads to an unstable structure. HSE relaxations from a number of the initial lattice structures where Be_i is placed next to the $V_{Ga}O_NBe_{Ga}$ complex, result in the Be atom relaxing back into the gallium vacancy, restoring the $Be_{Ga}O_NBe_{Ga}$ complex. In order to estimate the dissociation energy of the $Be_{Ga}O_NBe_{Ga}$ acceptor, we calculated the diffusion path of removal of Be atom from the complex to the next nearest interstitial site, using the nudged elastic band (NEB) method. NEB calculations were performed using the HSE parametrization of the deep polaronic state of the $Be_{Ga}O_NBe_{Ga}$ acceptor. This diffusion path along with the dissociation energy is shown in Fig. 15.

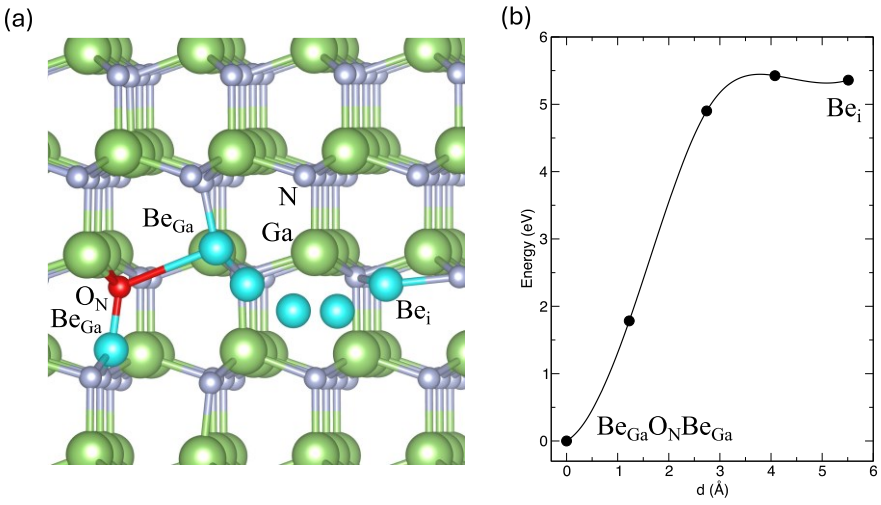

Fig. 15. Dissociation path of the $Be_{Ga}O_NBe_{Ga}$ complex in (a) GaN crystal lattice; i.e., moving Be_{Ga} to the next nearest Be_i, (b) HSE total energy along this path obtained using NEB.

While the binding energy of the $Be_{Ga}O_NBe_{Ga}$ complex is a relatively low 0.3 eV (with respect to isolated Be_{Ga} and $Be_{Ga}O_N$ dimer), the dissociation energy of this complex in bulk GaN is a large ~5.4 eV. In addition to the crystal lattice deformations that the dissociation requires, this is also due to the strong electrostatic interaction between the double donor Be_i^{2+} and a deep double acceptor V_{Ga}^{2-} which is left in place of the removed Be_{Ga}. Therefore, once the $Be_{Ga}O_NBe_{Ga}$ complex

is formed on the surface during GaN growth, it remains stable in the bulk of the material in the post-growth annealing and subsequent experiments at high temperatures.

The HSE calculated 0/– transition level of the deep polaronic state is at 0.34 eV above the VBM for a slightly more stable in-plane polaronic state of the acceptor. The shallow state is calculated to have the 0/– transition level at about 0.12 eV above the VBM. Therefore, HSE predicts the ground state of the hole localized on the $Be_{Ga}O_NBe_{Ga}$ acceptor is a deep in-plane polaron, while the shallow state is metastable. A weakly localized nature of the shallow state suggests a more efficient capture of the photogenerated hole by this state, compared to the strongly localized small polaron. In order to analyze the stability of a captured hole, we use the NEB method within HSE to calculate the energy pathway between the shallow and deep polaronic states. Koopmans tuned HSE for the deep polaronic state was used in this calculation. Since this parametrization of HSE does not fulfill the Koopmans' condition for the shallow state, total energy correction was applied to the shallow state to bring the total energy differences between the states in accord with the thermodynamic transition levels calculated by the appropriate HSE functionals. In addition, the shallow-state post-processing energy corrections were also applied to the intermediate states where the defect state wavefunctions retain shallow character. This energy path, along with the corresponding hole spin densities, are shown in Fig. 16.

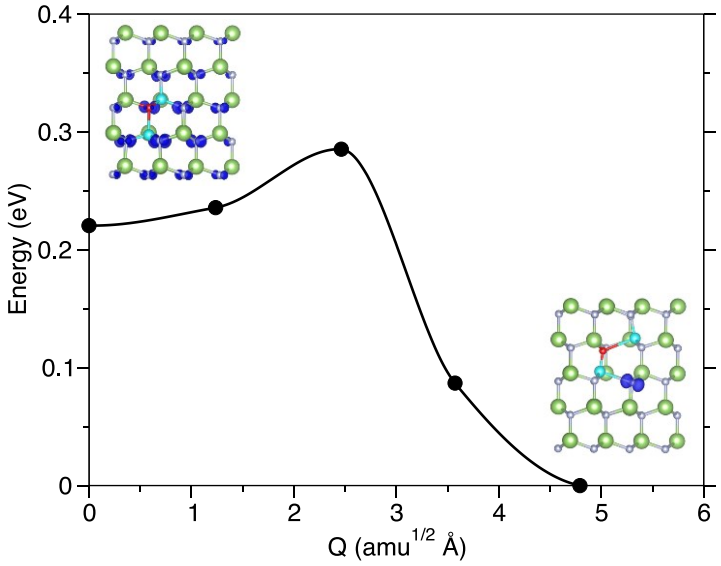

Fig. 16. Potential barrier path as a function of the defect configuration coordinate Q for the hole captured at the shallow state of $Be_{Ga}O_NBe_{Ga}$ acceptor towards the deep ground state of the in-plane small polaron. Corresponding hole spin densities are shown for reference.

HSE calculations predict a relatively low energy barrier of 0.065 eV for a photogenerated hole captured on the weakly localized shallow state to be transferred to the deep ground state. This barrier value suggests that the PL originating from the shallow state should be quenching at temperatures of around 30 K. In the PL experiments, the quenching of the UVL_{Be} band is observed at $T > 60$-90 K which suggests that this barrier is likely underestimated in HSE calculations. Details of PL kinetics and its dependence on the relative energies between the shallow and deep states are given in Sec. III.B.2.

HSE calculated optical transitions via $Be_{Ga}O_NBe_{Ga}$ acceptor are shown in Fig. 17, where configuration coordinate diagrams for the deep polaronic and shallow states of this defect are presented. In Fig. 17 the solid lines show adiabatic potentials obtained by fitting into HSE optical transition energies within the harmonic approximation. Solid symbols connected by dotted lines show adiabatic potentials obtained by the direct static HSE calculations in the Q-direction between

the relaxed neutral and 1– charge state lattices. Defect energies in each lattice configuration were corrected for the artificial interactions in the periodic supercells following Ref. 37. Deep polaronic and shallow states exhibit the resonant absorption of 3.45 eV and 3.4 eV, respectively, which are close to the bulk GaN bandgap of 3.50 eV. Absorption of a photon with the above bandgap energy creates an electron-hole pair, which upon thermalization end up in respective band edges (dashed $E(-)+E_g$ potential in Fig. 17). Subsequent nonradiative hole capture by the negatively charged $Be_{Ga}O_NBe_{Ga}$ acceptor into both shallow and deep states is predicted to be efficient, with no potential barrier for hole capture. However, the delocalized nature of the shallow state suggests a more efficient hole capture by the shallow state.

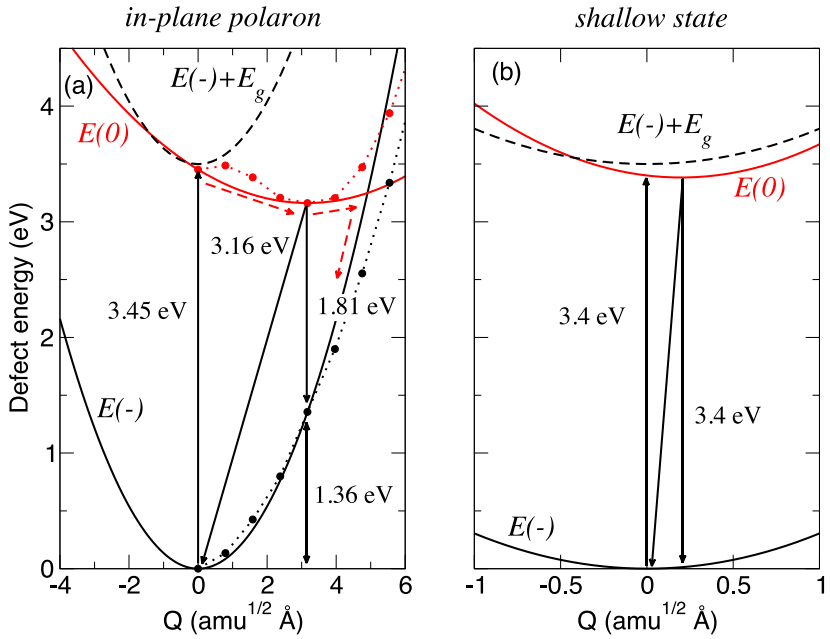

Fig. 17. Configuration coordinate diagram for (a) the deep polaronic and (b) shallow states of $Be_{Ga}O_NBe_{Ga}$ acceptor calculated with the Koopmans tuned HSE. Solid arrows show radiative optical transitions, and dashed arrows indicate the non-radiative transition path in the deep acceptor state. Solid lines show adiabatic potentials obtained by fitting within harmonic approximation into HSE optical transition energies. Filled symbols show direct HSE calculations of the series of defect lattice geometries along the Q-direction connecting the relaxed neutral and 1– lattice structures.

For the neutral deep state, we obtain two contradictory results regarding the possible radiative or non-radiative nature of the deep polaronic state of the $Be_{Ga}O_NBe_{Ga}$ acceptor. On the one hand, the barrier for the non-radiative electron-hole recombination (dashed arrows in Fig. 17(a)) obtained from the fitted adiabatic potentials (solid lines) is a low 0.08 eV. This suggests that the localized polaronic state of the $Be_{Ga}O_NBe_{Ga}$ acceptor could be non-radiative. On the other hand, adiabatic potentials obtained by direct static HSE calculations (filled symbols with dotted lines) suggest a somewhat anharmonic potential in the neutral polaronic state and a large potential barrier for the nonradiative recombination of about 1.5 eV. It remains an open question whether a different vibrational mode exists for the deep polaronic state of the $Be_{Ga}O_NBe_{Ga}$ acceptor, which would allow for nonradiative recombination via this defect. In either case, if the barrier between the shallow and deep states is low for a thermal jump, the photogenerated hole is initially captured by the shallow state, then transfers to the deep polaronic state, and recombines with the electron from the conduction band (or a shallow donor) radiatively or non-radiatively. Radiative transitions associated with the deep state are expected to produce a broad red PL with a maximum at 1.81 eV and ZPL at 3.16 eV. In the following, we will consider both possibilities for electron-hole recombination via the deep states – radiative with a PL band at ~1.8 eV and nonradiative.

The shallow state of the $Be_{Ga}O_NBe_{Ga}$ acceptor, on the other hand, does not exhibit a possible non-radiative recombination pathway, i.e., the $E(0)$ and $E(-)+E_g$ adiabatic potentials do not intersect. Therefore, at low temperatures, where the hole captured by the shallow state does not transfer to the deep state, HSE calculations predict a sharp UVL band with ZPL at 3.38 eV and PL maximum at 3.4 eV (Fig. 17(b)). In comparison with the UVL band produced by the isolated Be_{Ga} acceptor (HSE calculated transition level is 0.18 eV),[37] the UVL band produced by the $Be_{Ga}O_NBe_{Ga}$ acceptor is sharper, with calculated Franck-Condon shift of ~0.01 eV, which is at the

limit of accuracy of HSE defect energy calculations. This low value of the Franck-Condon shift is due to a low ΔQ = 0.2 amu^{½}Å displacement between the relaxed neutral shallow state and negatively charged defect lattice geometries. The Franck-Condon shift of the isolated Be_{Ga} was calculated at a slightly larger 0.05 eV. Therefore, HSE-calculated PL parameters suggest that $Be_{Ga}O_NBe_{Ga}$ exhibits an acceptor level that is shallower than that of the isolated Be_{Ga}.

The HSE-calculated vibrational parameters for the shallow state of the $Be_{Ga}O_NBe_{Ga}$ acceptor are as follows. The vibrational energies of the ground $E(-)$ and excited $E(0)$ states, calculated along the Q-direction connecting the two relaxed defect lattice geometries are 51 and 61 meV, respectively. The corresponding ground and excited states' Huang-Rhys factors are 0.24 and 0.28. For the deep polaronic state, vibrational energies of the ground $E(-)$ and excited $E(0)$ states are 34 and 16 meV, respectively (within harmonic approximation as shown by solid adiabatic potentials in Fig. 17 (a)). The corresponding ground and excited states' Huang-Rhys factors are 40 and 19.

2. Phenomenological model

Temperature dependences of PL intensities associated with shallow and deep states of a dual-nature acceptor can be simulated by using the rate equation model.[25,37] The internal quantum efficiencies (IQEs) of electron-hole recombinations (radiative or nonradiative) via the deep-state (η_D) and shallow-state (η_S) should have the following dependence on temperature [37]

$$\eta_D(T) = \frac{\tau_{D\to S}}{\tau_{n\to D}} \frac{B\eta_D(0) + \eta_S(0)}{AB - 1}\ , \tag{5}$$

$$\eta_S(T) = \frac{\tau_{D\to S}}{\tau_{n\to S}} \frac{\eta_D(0) + A\eta_S(0)}{AB - 1}\ , \tag{6}$$

where $A = 1 + \tau_{D\to S}\left(1/\tau_{n\to D} + 1/\tau_{D,therm}\right)$ and $B = 1 + \tau_{S\to D}\left(1/\tau_{n\to S} + 1/\tau_{S,therm}\right)$; $\eta_D(0)$ and $\eta_S(0)$ are IQEs for the deep and shallow states, respectively, at $T \to 0$; $\tau_{n\to D}$ and $\tau_{n\to S}$ are PL (or nonradiative recombination) lifetimes for the deep and shallow states; $\tau_{D\to S} = \nu_D^{-1}\exp\left(E_{DS}/kT\right)$ and $\tau_{S\to D} = \nu_S^{-1}\exp\left(E_{SD}/kT\right)$ are transfer times from the deep to shallow ($D\to S$) or shallow to deep ($S\to D$) states with vibrational frequencies ν_D and ν_S over barriers E_{DS} and E_{SD}, respectively. The characteristic times of thermal emission of holes from the deep and shallow states to the valence band ($\tau_{D,therm}$ and $\tau_{S,therm}$) are: $\tau_{D,therm} = \left(C_{pD}N_v\right)^{-1} g\exp\left(E_D/kT\right)$ and $\tau_{S,therm} = \left(C_{pS}N_v\right)^{-1} g\exp\left(E_S/kT\right)$, where C_{pD} and C_{pS} are the hole-capture coefficients for the deep and shallow states; E_D and E_S are the energies of the deep and shallow –/0 transition levels above the VBM, g is the degeneracy factor, and N_v is the effective density of states in the valence band.

Examples of calculated $\eta_D(T)$ and $\eta_S(T)$ dependences for electron-hole recombination via the deep and shallow states of the proposed $Be_{Ga}O_NBe_{Ga}$ complex are shown in Fig. 18. According to first-principles calculations in Sec. IIIB1, E_D = 0.34 eV, E_S = 0.12 eV, E_{DS} = 0.285 eV, and E_{SD} = 0.065 eV. Other parameters were presumed in this example (given in the caption of Fig. 18).

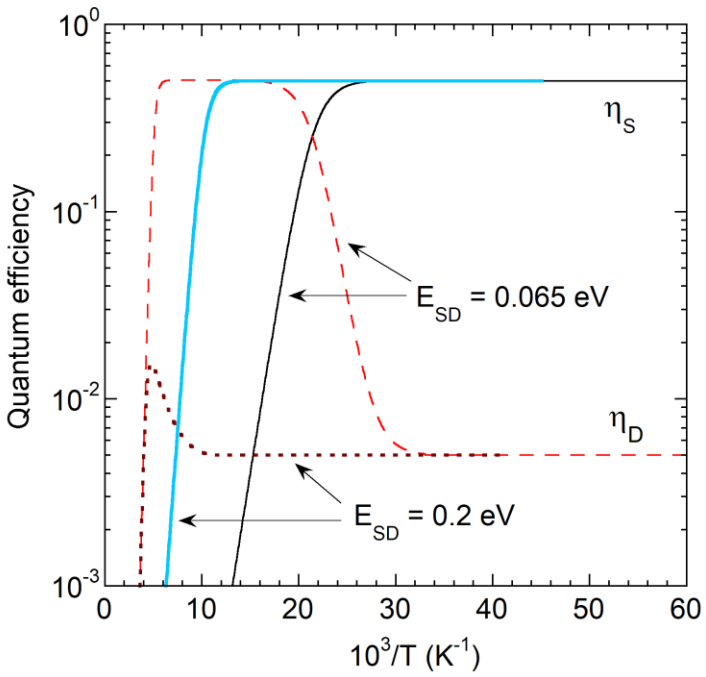

Fig. 18. Temperature dependences of IQE for electron-hole recombination via the shallow (η_S) and deep (η_D) states of the $Be_{Ga}O_NBe_{Ga}$ acceptors in GaN calculated using Eqs. (5) and (6) with the following parameters: E_D = 0.34 eV, E_S = 0.12 eV, C_{pD} = 10^{-8} cm^3/s, C_{pS} = 10^{-6} cm^3/s, $\tau_{n\to D}$ = 10^{-4} s, $\tau_{n\to S}$ = 10^{-6} s, ν_D = ν_S = 10^{13} s^{-1}, $\eta_D(0)$ + $\eta_S(0)$ = 0.5. Two sets of dependences are shown: for the HSE-calculated barriers (E_{SD} = 0.065 eV, E_{DS} = 0.285 eV) and for higher barriers (E_{SD} = 0.20 eV, E_{DS} = 0.42 eV) between the shallow and deep states.

Let us first consider predictions of the phenomenological model (with HSE-calculated parameters) and assume that recombination via the deep state is radiative (if it is nonradiative, just replace "PL" with "nonradiative recombination efficiency"). At low temperatures (T < 25-30 K), the PL from the shallow state is stronger than from the deep state by a factor of C_{pS}/C_{pD}. We anticipate that the shallow state captures holes more efficiently and, therefore, $C_{pS} >> C_{pD}$. With increasing temperature, holes at the shallow level get enough energy to overcome the potential barrier E_{SD}. Then, the PL intensity from the shallow state decreases with temperature as $\exp(E_{SD}/kT)$, and the PL intensity from the deep state increases with the same slope. At temperatures between 50 and 200 K, only PL from the deep state would be observed. At higher

temperatures, the PL quenching with the activation energy equal to $E_D = 0.34$ eV should occur due to the thermal emission of holes from the deep state to the valence band. The PL intensity from the shallow state is expected to increase at temperatures above 150 K due to the thermal emission of holes from the deep ground state into the shallow state (this mechanism was explained in Ref. 25), but its IQE remains below 10^{-5} (not shown in Fig. 18) because of relatively large value of $\Delta E = E_D - E_S$.

The PL lifetimes, $\tau_{n\to D} = 100$ μs and $\tau_{n\to S} = 1$ μs, were assumed according to typical values of C_n for acceptors in GaN (Fig. 6). Note that increasing or decreasing $\tau_{n\to S}$ by a factor of 10 only slightly shifts critical temperature T_0 at which the quenching of PL from the shallow state begins (between 40 and 55 K) but does not affect PL IQEs in regions where they are independent of temperature. Moreover, the temperature dependences at $T < 150$ K are insensitive to $\tau_{n\to D}$ (for $\tau_{n\to D}$ between 10^{-10} and 1 s). In particular, if the electron-hole recombination via the deep state is nonradiative, the temperature dependence of the nonradiative recombination efficiency at $T < 150$ K would be the same as shown with the dashed curve in Fig. 18. Since the total IQE of the recombination via the $Be_{Ga}O_NBe_{Ga}$ acceptor is much smaller than unity, such variations in the nonradiative recombination with temperature would remain unnoticed in the PL experiment.

In the above example, the barrier for the shallow-to-deep state transition is relatively small ($E_{SD} < E_S$), the quenching of PL from the shallow state occurs without emission of holes to the valence band, and the IQE of the emerged PL from the deep state (or nonradiative recombination efficiency) must be the same as that of the shallow state. Alternatively, if the barrier is large ($E_{SD} > E_S$), the quenching of the shallow-state-related PL would begin due to the thermal emission of holes to the valence band (at critical temperature $T_0 \approx 90$ K in Fig. 18 for any $E_{SD} > E_S$). In this

case, the PL from the deep state may remain unnoticed in PL experiments even if this recombination is radiative.

IV. DISCUSSION

We have established that the UVL_{Be} band with the strongest peak at about 3.38 eV in Be-doped GaN is caused by an acceptor with the –/0 transition level at 0.113 eV above the VBM. This acceptor cannot be an isolated Be defect such as Be_{Ga}, Be_N, or Be_i.[63] On the other hand, it can be found only in GaN samples with relatively high concentrations of Be (above 10^{17} cm^{-3}). These findings indicate that it must be a Be-containing complex. Our first-principles calculations show that the only candidate for such a shallow acceptor (besides Be_{Ga}) is the $Be_{Ga}O_NBe_{Ga}$ complex if we limit the number of the defect components to three. Note that according to HSE calculations, the $Be_{Ga}O_N$ is a deep donor,[64] or it does not have transition levels in the bandgap,[63] but it cannot be a shallow acceptor.

From our HSE calculations, the $Be_{Ga}O_NBe_{Ga}$ complex is a dual-nature acceptor. The shallow level with a delocalized hole is predicted at 0.12 eV, and the deep polaronic state – at 0.34 eV above the VBM. Theory predicts a potential barrier E_{SD} = 0.065 eV for the transition of a bound hole from the shallow state to the deep one. At first glance, such a potential barrier could explain why PL from the shallow state (the UVL_{Be} band) is observed at low temperatures, in contrast to the case of the isolated Be_{Ga} acceptor, where this barrier is smaller than 20 meV.[25] However, the phenomenological model (Sec. IIIB2) predicts the quenching of the UVL_{Be} band at $T > 30$ K with the activation energy of E_{SD} = 65 meV and the concurrent emergence of a broad PL band with a maximum near 1.8 eV (it would not be observed if the recombination via the deep state is nonradiative). In experiments, the quenching of the UVL_{Be} band is observed at $T >$ 60-90 K with an activation energy of 60-95 meV. Most likely, this quenching is caused by the thermal emission

of holes from the –/0 level to the valence band. A slightly smaller activation energy in the Arrhenius plot than E_A = 113 meV is due to several reasons and is typical for defects in GaN.[55] Importantly, the characteristic temperature of the quenching is tunable by the excitation intensity and not abrupt, which agrees with the predictions of the phenomenological model.[56] This finding excludes the possibility that the quenching is caused by the escape of the holes from the shallow state to the deep one. We conclude that the barrier from the shallow state to the deep state is likely higher than 0.1 eV.

To date, the dual nature of cation-site acceptors was confirmed experimentally only for the isolated Be_{Ga} defect in GaN.[25] In particular, the polaronic state is predicted for the Mg_{Ga} acceptor,[24,65-67] but only the shallow state is observed as the UVL_{Mg} band in GaN.[68] This apparent contradiction could be resolved if the deep and shallow levels of Mg_{Ga} coincide (with an accuracy of about 10 meV) and the potential barrier between these two states is at least 50 meV.[25,37] The same restrictions may explain why PL from the deeper state is not observed in experiments for the Zn_{Ga} acceptor.[37] According to calculations of the current study, the $Be_{Ga}O_NBe_{Ga}$ acceptor has a radiative shallow state at 0.12 eV (responsible for the UVL_{Be} band with a maximum at 3.38 eV) and a deep polaronic state at ~0.34 eV (radiative or nonradiative), which could not be found in PL experiments. Note that the deep state of the $Be_{Ga}O_NBe_{Ga}$ acceptor is predicted to have the same energy above the VBM as the Be_{Ga} acceptor, and the latter's concentration greatly exceeds the former's concentration**.** Therefore, it may not be possible to confirm its existence by other experiments such as deep-level transient spectroscopy. For the verification of the polaronic state of the $Be_{Ga}O_NBe_{Ga}$ acceptor predicted at 0.34 eV, experiments with Be-O co-doping are promising. We expect that the co-doping of GaN with Be and O may lead to an abundance of the $Be_{Ga}O_NBe_{Ga}$ acceptors so that their concentration will exceed the concentration of compensating donors.

The idea of co-doping is not new.[69] More than 25 years ago, Yamamoto and Katayama-Yoshida predicted that co-doping of GaN with acceptors A and shallow donors D would lead to the formation of the tri-component (ADA) complexes that would have the shallowest ionization energies.[70,71] It was suggested that Be or Mg as acceptors (A) and Si or O as shallow donors (D) form tri-complexes that are shallow acceptors. Since then, several experimental works demonstrated high *p*-type conductivity in GaN co-doped with Mg and O,[9,10,11] co-doped with Be and O,[72,73] and GaN co-implanted with Be and O.[74,75] By co-doping GaN and $Al_xGa_{1-x}N$ ($x = 0.4$) with Mg (A) and Si (D), Aoyagi et al.[76] demonstrated high hole carrier concentrations ($p = 2\times10^{19}$ and 6×10^{18} cm^{-3}, respectively). Finally, first-principles calculations show that the triplet $Mg_{Al}O_NMg_{Al}$ complex in AlN is a shallower acceptor ($E_A = 0.34$ eV) than the isolated Mg_{Al} ($E_A = 0.50$ eV).[77]

Finally, we would like to address questions raised in Sec. IIIA: Why is the UVL_{Be} band very weak or absent in *n*-type GaN:Be samples, and why is thermal annealing necessary for the $Be_{Ga}O_NBe_{Ga}$ activation in MBE-grown GaN:Be? While it may seem counterintuitive, experiments show that complexes involving several components are abundant in semiconductors. Examples include tri-carbon complexes with concentrations higher than 10^{18} cm^{-3} in C-doped GaN,[78,79,80] and four-component complexes in Si.[81] In our MOCVD GaN:Be samples, the typical concentration of oxygen is 10^{17}-10^{18} cm^{-3}. The Be and O species are immobile in bulk GaN at growth temperatures (970 °C for our MOCVD growth).[82] One possibility is that the $Be_{Ga}O_NBe_{Ga}$ complexes are formed at the surface during the growth and remain buried. Alternatively, high concentrations of mobile gallium vacancies may facilitate the formation of the complexes during growth in nitrogen-rich conditions. Further, hydrogen atoms may participate in forming the $Be_{Ga}O_NBe_{Ga}$ complexes. This assumption can explain why the UVL_{Be} band is usually observed in

semi-insulating GaN but is very weak or absent in conductive *n*-type GaN. Indeed, hydrogen in interstitial sites (H_i) is positively charged and very mobile when the Fermi level is in the lower part of the GaN bandgap, and it is negatively charged and immobile at 1000 °C in *n*-type GaN when the Fermi level is close to the conduction band.[58,83-85] The exact role of hydrogen in forming the $Be_{Ga}O_NBe_{Ga}$ complexes is unknown, and further experiments with thermal annealing in hydrogen-rich and hydrogen-free ambients may shed light on this issue. Nitrogen vacancies may affect the formation of the $Be_{Ga}O_NBe_{Ga}$ complexes, especially in GaN:Be grown in Ga-rich conditions. The V_N donors may passivate the $Be_{Ga}O_NBe_{Ga}$ acceptors during the growth, while post-growth thermal annealing may activate them. This mechanism can explain why the UVL_{Be} band emerges in MBE-grown GaN:Be samples (grown under Ga-rich conditions) only at $T_{ann} > 700$ °C (Sec. IIIA5).

V. CONCLUSION

The shallowest acceptor in GaN, with an ionization energy of 113 meV, is attributed to the $Be_{Ga}O_NBe_{Ga}$ complex. This attribution is based on a detailed analysis of photoluminescence results and first-principles calculations. The dual nature of this acceptor is predicted theoretically, but no confirmation of it has been currently found in the experimental data. Co-doping of GaN with Be and O may result in conductive *p*-type GaN. Understanding co-doping mechanisms may also lead to breakthroughs in doping ultrawide-bandgap nitride semiconductors.

Acknowledgments

The work at VCU and SUNY was partly supported by the National Science Foundation under grants DMR-2423874 and DMR-2423875, respectively. The calculations were performed at the VCU High Performance Research Computing (HPRC) core facility.

Conflict of Interest

The authors have no conflicts to disclose.

Data Availability Statement

The data supporting this study's findings are available from the corresponding author upon reasonable request.

Keywords

Photoluminescence, GaN, point defects, complexes, semiconductors.

References

[1] H. Morkoç, *Handbook of Nitride Semiconductors and Devices* (Wiley, New York, 2008).

[2] E. Rocco, J. Marini, K. Hogan, V. Meyers, B. Mcewen, L. D. Bell, and F. Shahedipour-Sandvik, "Overview and Progress Toward High-Efficiency, Air Stable, Cs-Free III Nitride Photocathode Detectors", IEEE Photonics J. **14**, 6818312 (2022).

[3] G. Li, W. Wang, W. Yang, Y. Lin, H. Wang, Z. Lin, and S. Zhou, "GaN-based light-emitting diodes on various substrates: a critical review", Rep. Prog. Phys. **79**, 056501 (2016).

[4] E. A. Jones, F. Wang, and D. Costinett, "Review of Commercial GaN Power Devices and GaN-Based Converter Design Challenges", IEEE J. Emerging Selected Topics in Electronics, **4**, 707-719 (2016).

[5] J. Simon, V. Protasenko, C. Lian, H. Xing, D. Jena, "Polarization-Induced Hole Doping in Wide-Band-Gap Uniaxial Semiconductor Heterostructures", Science **327**, 60-64 (2010).

[6] K. Ebata, J. Nishinaka, Y. Taniyasu, and K. Kumakura, "High hole concentration in Mg-doped AlN/AlGaN superlattices with high Al content", Jap. J. Appl. Phys. **57**, 2-5 (2018).

[7] C. J. Zollner, S. P. DenBaars, J. S. Speck, and S. Nakamura, "Germicidal ultraviolet LEDs: a review of applications and semiconductor technologies", Semicond. Sci. Technol. **36**, 123001 (2021).

[8] S. Nikishin, A. Bernussi, and S. Karpov, "Towards Efficient Electrically-Driven Seep UVC Lasing: Challenges and Opportunities", Nanomaterials **13**, 185 (2023).

[9] R. Y. Korotkov, J. M. Gregie, and B. W. Wessels, "Electrical properties of p-type GaN:Mg codoped with oxygen*",* Appl. Phys. Lett. **78**, 222-224 (2001).

[10] G. Kipshidze, V. Kuryatkov, B. Borisov, Y. Kudryavtsev, R. Azomoza, S. Nikishin, and H. Temkin, "Mg and O cooping in p-type GaN and $Al_xGa_{1-x}N$ ($0<x<0.08$)", Appl. Phys. Lett. **80**, 2910-2912 (2002).

[11] A. G. Jacobs, J. A. Spencer, J. K. Hite, K. D. Hobart, T. J. Anderson, and B. N. Feigelson, "Novel Codoping Moiety to Achieve Enhanced p-Type Doping in GaN by Ion Implantation". Phys. Stat. Sol. A 2200848 (2023).

[12] S. Sugita, Y. Watari, G. Yoshizawa, J. Sodesawa, H. Yamamizu, K.-T. Liu, Y.-K. Su, and Y. Horikoshi, "Growth of Be-doped p-type GaN under invariant polarity conditions", Jpn. J. Appl. Phys. **42**, 7194-7197 (2003).

[13] Z.-C. Feng, Y. J. Sun, L. S. Tan, S. J. Chua, J. W. Yu, C. C. Yang, W. Lu, and W. E. Collins, "P-type doping in GaN through Be implantation", Phys. Stat. Sol. (c) **2**, 2415-2419 (2005).

[14] C.-C. Yu, C.-F. Chu, J.-Y. Tsai, C.-F. Lin, W.-H. Lan, C.-I. Chiang, and S.-C. Wang, "Be-implanted p-type GaN with high carrier concentration", Jap. J. Appl. Phys. **40**, L417-L419 (2001).

[15] T. M. Al Tahtamouni, A. Sedhain, J. Y. Lin and H. X. Jiang, "Beryllium Doped *p*-type GaN Grown by Metal-Organic Chemical Vapor Deposition", Jordan J. Physics **3**, 77-81 (2010).

[16] A. Salvador, W. Kim, O. Aktas, A. Botchkarev, Z. Fan, and H. Morkoc, "Near ultraviolet luminescence of Be doped GaN grown by reactive molecular beam epitaxy using ammonia", Appl. Phys. Lett. **69**, 2692-2694 (1996).

[17] H. Ahmad, J. Lindemuth, Z. Engel, C. M. Matthews, T. M. McCrone, and W. A. Doolittle, "Substantial P-Type Conductivity of AlN Achieved via Beryllium Doping", Adv. Mater. **33**, 2104497 (2021).

[18] W. A. Doolittle, C. M. Matthews, H. Ahmad, S. Lee, A. Ghosh, E. N. Marshall, A. L. Tang, P. Manocha, and D. Yoder, "Prospectives for AlN electronics and optoelectronics and the important role of alternative synthesis", Appl. Phys. Lett. **123**, 070501 (2023).

[19] H. Ahmad, Z. Engel, C. M. Matthews, S. Lee, and W. A. Doolittle, "Realization of homojunction PN AlN diodes", J. Appl. Phys. **131**, 175701 (2022).

[20] D. J. Dewsnip, A. V. Andrianov, I. Harrison, J. W. Orton, D. E. Lacklison, G. B. Ren, S. E. Hooper, T. S. Cheng, and C. T. Foxon, "Photoluminescence of MBE grown wurtzite Be-doped GaN", Semicond. Sci. Technol. **13**, 500 (1998).

[21] F. J. Sánchez, F. Calle, M. A. Sánchez-García, E. Calleja, E. Muñoz, C. H. Molloy, D. J. Somerford, J. J. Serrano, and J. M. Blanco, "Experimental evidence for a Be shallow acceptor in GaN grown on Si(111) by molecular beam epitaxy", Semicond. Sci. Technol. **13**, 1130-1133 (1998).

[22] K. Lee, B. L. VanMil, M. Luo, L. Wang, N. C. Giles, and T. H. Myers, "Thermal activation of beryllium-related photoluminescence by annealing of GaN grown by molecular beam epitaxy", Phys. Stat. Solidi (c) **2**, 2204-2207 (2005).

[23] D. O. Demchenko, M. Vorobiov, O. Andrieiev, T. H. Myers, and M. A. Reshchikov, "Shallow and deep states of beryllium acceptor in GaN: Why photoluminescence experiments do not reveal small polarons for defects in semiconductors", Phys. Rev. Lett. **126**, 027401 (2021).

[24] S. Lany and A. Zunger, "Dual nature of acceptors in GaN and ZnO: The curious case of the shallow Mg_{Ga} deep state", Appl. Phys. Lett. **96**, 142114 (2010).

[25] M. A. Reshchikov, M. Vorobiov, O. Andrieiev, D. O. Demchenko, B. McEwen, and F. Shahedipour-Sandvik, "Dual Nature of the Be_{Ga} Acceptor in GaN: Evidence from Photoluminescence", Phys. Rev. B **108**, 075202 (2023).

[26] J. L. Lyons, A. Janotti, and C. G. Van de Walle, "Impact of group-II acceptors on the electrical and optical properties of GaN", Jap. J. Appl. Phys. **52**, 08JJ04 (2013).

[27] X. Cai, J. Yang, P. Zhang, and S.-H. Wei, "Origin of Deep Be Acceptor Levels in Nitride Semiconductors: The Roles of Chemical and Strain Effects", Phys. Rev. Appl. **11**, 034019 (2019).

[28] S. Jin, X. Li, W. Yang, Y. Zhao, L. Bian, S. Lu, "Electrical and Optical Properties of Beryllium Deep Acceptors in GaN", J. Electron. Mater. **49**, 7472-7478 (2020).

[29] S. Qiao, Y.-N. Wu, X. Yan, B. Monserrat, S.-H. Wei, and B. Huang, "Temperature effect on charge-state transition levels of defects in semiconductors", Phys. Rev. B **105**, 115201 (2022).

[30] K. Lee, "Issues for p-type doping of gallium nitride with beryllium and magnesium grown by rf-plasma assisted molecular beam epitaxy", Ph.D., West Virginia University, United States – West Virginia (2007).

[31] A. J. Ptak, T. H. Myers, L. Wang, N. C. Giles, M. Moldovan, C. R. Da Cunha, L. A. Hornak, C. Tian, R. A. Hockett, S. Mitha, and P. Van Lierde, "A Comparison of Magnesium and Beryllium Acceptors in GaN Grown by rf-Plasma Assisted Molecular Beam Epitaxy", MRS Online Proc. Library **639**, 33 (2000). 10.1557/PROC-639-G3.3

[32] M. A. Reshchikov, "Measurement and analysis of photoluminescence in GaN", J. Appl. Phys. **129**, 121101 (2021).

[33] M. A. Reshchikov, M. A. Foussekis, J. D. McNamara, A. Behrends, A. Bakin, and A.Waag, "Determination of the absolute internal quantum efficiency of photoluminescence in GaN co-doped with Zn and Si", J. Appl. Phys. **111**, 073106 (2012).

[34] M. A. Reshchikov, A. A. Kvasov, M. F. Bishop, T. McMullen, A. Usikov, V. Soukhoveev, and V. A. Dmitriev, "Tunable and abrupt thermal quenching of photoluminescence in high-resistivity Zn-doped GaN", Phys. Rev. B **84**, 075212 (2011).

[35] M. A. Reshchikov, M. Vorobiov, D. O. Demchenko, Ü. Özgür, H. Morkoç, A. Lesnik, M. P. Hoffmann, F. Hörich, A. Dadgar, and A. Strittmatter, "Two charge states of the C_N acceptor in GaN: Evidence from photoluminescence", Phys. Rev. B **98**, 125207 (2018).

[36] J. Heyd, G. E. Scuseria, and M. Ernzerhof, "Hybrid Functionals Based on a Screened Coulomb Potential", J. Chem. Phys. **118**, 8207–8215 (2003).

[37] D. O. Demchenko, M. Vorobiov, O. Andrieiev, M. A. Reshchikov, B. McEwen, and F. Shahedipour-Sandvik, "Koopmans-tuned Heyd-Scuseria-Ernzerhof hybrid functional calculations of acceptors in GaN", Phys. Rev. B **110**, 035203 (2024).

[38] A. Alkauskas, Q. Yan, and C. G. Van de Walle, "First-principles theory of nonradiative carrier capture via multiphonon emission", Phys. Rev. B **90**, 075202 (2014).

[39] F. Williams, "Donor-Acceptor Pairs in Semiconductors", Phys. Stat. Sol. **25**, 493-512 (1968).

[40] M. A. Reshchikov, M. Vorobiov, O. Andrieiev, B. McEwen, E. Rocco, V. Meyers, D. O. Demchenko, and F. Shahedipour-Sandvik, "Photoluminescence from Be-Doped GaN Grown by Metal-Organic Chemical Vapor Deposition", Phys. Stat. Sol. (b) **260**, 2200487 (2023).

[41] M. A. Reshchikov, O. Andrieiev, M. Vorobiov, D. O. Demchenko, B. McEwen, and F. Shahedipour-Sandvik, "Photoluminescence from GaN implanted with Be and F", Phys. Stat. Sol. B **260**, 2300131 (2023).

[42] T. Kamiya and E. Wagner, "Optical determination of impurity compensation in n-type gallium arsenide", J. Appl. Phys. **48**, 1928-1934 (1977).

[43] N. Pan, S. S. Bose, M. H. Kim, G. E. Stillman, F. Chambers, G. Devane, C. R. Ito, and M. Feng, "Hydrogen passivation of C acceptors in high-purity GaAs", Appl. Phys. Lett. **51**, 596-598 (1987).

[44] M. A. Reshchikov and H. Morkoç, "Luminescence properties of defects in GaN", J. Appl. Phys. **97**, 061301 (2005).

[45] K. Kornizer, T. Ebner, K. Thonke, R. Sauer, C. Kirchner, V. Schwegler, M. Kamp, M. Leszczynski, I. Grzegory, and S. Porowski, "Photoluminescence and reflectance spectroscopy of excitonic transitions in high-quality homoepitaxial GaN films", Phys. Rev. B **60**, 1471-1473 (1999).

[46] M. A. Reshchikov, J. D. McNamara, F. Zhang, M. Monavarian, A. Usikov, H. Helava, Yu. Makarov, and H. Morkoç, "Zero-phonon line and fine structure of the yellow luminescence band in GaN", Phys. Rev. B **94**, 035201 (2016).

[47] W. J. Moore, J. A. Freitas, Jr., S. K. Lee, S. S. Park, and J. Y. Han, "Magneto-optical studies of free-standing hydride-vapor-phase epitaxial GaN", Phys. Rev. B **65**, 081201 (2002).

[48] E. Zacks and A. Halperin, "Dependence of the peak energy of the pair photoluminescence band on excitation intensity", Phys. Rev. B **6**, 3072-3075 (1972).

[49] D. G. Thomas, J. J. Hopfield, and W. M. Augustyniak, "Kinetics of Radiative Recombination at Randomly Distributed Donors and Acceptors", Phys. Rev. **140**, A202-A220 (1965).

[50] R. Dingle and M. Ilegems, "Donor-acceptor pair recombination in GaN", Sol. St. Commun. **9**, 175-180 (1971).

[51] M. Jaworek, A. Wysmolek, M. Kaminska, A. Twardowski, M. Bockowski, and I. Grzegory, "Photoluminescence Study of Bulk GaN Doped with Beryllium", Acta Physica Polonica A **108**, 705-710 (2005).

[52] K. Huang and A. Rhys, "Theory of light absorption and non-radiative transitions in F-centers", Proc. R. Soc. A **204**, 406-423 (1950).

[53] A. M. Stoneham, *Theory of Defects in Solids*, Oxford University Press, Oxford, Great Britain, 1975, p. 315.

[54] A. Alkauskas, B. B. Buckley, D. D. Awschalom, and C. G. Van de Walle, "First-principles theory of the luminescence lineshape for the triplet transition in diamond NV centres", New J. Phys. **16**, 073026 (2014).

[55] M. A. Reshchikov, "Mechanisms of thermal quenching of defect-related luminescence in semiconductors", Phys. Stat. Sol. A **218**, 2000101 (2020).

[56] M. A. Reshchikov, "Two-step thermal quenching of photoluminescence in Zn-doped GaN", Phys. Rev. B **85**, 245203 (2012).

[57] M. A. Reshchikov, O. Andrieiev, M. Vorobiov, D. O. Demchenko, B. McEwen, and F. Shahedipour-Sandvik, "Photoluminescence from Cd_{Ga} and Hg_{Ga} acceptors in GaN", J. Appl. Phys. **135**, 155706 (2024).

[58] M. A. Reshchikov, O. Andrieiev, M. Vorobiov, B. McEwen, F. Shahedipour-Sandvik, D. Ye, and D. O. Demchenko, "Stability of the C_NH_i complex and the BL2 luminescence band in GaN", Phys. Stat. Sol. (b) **258**, 2100392 (2021).

[59] M. A. Reshchikov, D. Huang, F. Yun, P. Visconti, L. He, J. Jasinski, Z. Liliental-Weber, R. J. Molnar, and H. Morkoç "Unusual luminescence lines in GaN", J. Appl. Phys. **94**, 5623-5632 (2003).

[60] D. O. Demchenko and M. A. Reshchikov, "Hydrogen passivation of the beryllium acceptor in GaN and a possible route for *p*-type doping", Appl. Phys. Lett. **118**, 142103 (2021).

[61] H. Teisseyre, I. Gorczyca, N. E. Christensen, A. Svane, F. B. Naranjo, and E. Calleja, "Pressure behavior of beryllium-acceptor level in gallium nitride", J. Appl. Phys. **97**, 043704 (2005).

[62] M. A. Reshchikov, D. O. Demchenko, J. D. McNamara, S. Fernández-Garrido, and R. Calarco, "Green luminescence in Mg-doped GaN", Phys. Rev. B **90**, 035207 (2014).

[63] M. Vorobiov, O. Andrieiev, D. O. Demchenko, and M. A. Reshchikov, "Point Defects in Beryllium Doped GaN", Phys. Rev B **104**, 245203 (2021).

[64] H. Teisseyre, J. L. Lyons, A. Kaminska, D. Jankowski, D. Jarosz, M. Boćkowski, A. Suchocki, and C. G. Van de Walle, "Identification of yellow luminescence centers in Be-doped GaN through pressure-dependent studies", J. Phys. D: Appl. Phys. **50**, 22LT03 (2017).

[65] J. L. Lyons, A. Janotti, and C. G. Van de Walle, "Shallow versus Deep Nature of Mg Acceptors in Nitride Semiconductors", Phys. Rev. Lett. **108**, 156403 (2012).

[66] G. Miceli and A. Pasquarello, "Self-compensation due to point defects in Mg-doped GaN", Phys. Rev. B **93**, 165207 (2016).

[67] Y. Y. Sun, T. A. Abtew, P. Zhang, and S. B. Zhang, "Anisotropic polaron localization and spontaneous symmetry breaking: Comparison of cation-site acceptors in GaN and ZnO", Phys. Rev. B **90**, 165301 (2014).

[68] M. A. Reshchikov, P. Ghimire, and D. O. Demchenko, "Magnesium acceptor in gallium nitride: I. Photoluminescence from Mg-doped GaN", Phys. Rev. B **97**, 205204 (2018).

[69] J. Zhang, K. Tse, M. Wong, Y. Zhang, and J. Zhu, "A brief review of co-doping", Front. Phys. **11**, 117405 (2016).

[70] T. Yamamoto and H. Katayama-Yoshida, "Electronic structures of p-type GaN codoped with Be or Mg as the acceptors and Si or O as the donor codopants", J. Crystal Growth **189-190**, 532-536 (1998).

[71] H. Katayama-Yoshida, R. Kato, and T. Yamamoto, "New valence control and spin control method in GaN and AlN by codoping and transition atom doping", J. Crystal Growth **231**, 428-436 (2001).

[72] K. H. Ploog and O. Brandt, "Doping of group III nitrides", J. Vac. Sci. Technol. A **16**, 1609-01614 (1997).

[73] O. Brandt, H. Yang, H. Kostial, and K. H. Ploog "High *p*-type conductivity in cubic GaN/GaAs(113)*A* by using Be as the acceptor and O as the codopant", Appl. Phys. Lett. **69**, 2707-2709 (1996).

[74] Y. Nakano, T. Kachi, and T Jimbo, "Effect of Be^{+}+O^{+} coimplantation on Be acceptors in GaN", Appl. Phys. Lett. **82**, 2082-2084 (2003).

[75] D. G. Kent, M. E. Overberg, and S. J. Pearton, "Co-implantation of Be+O and Mg+O into GaN", J. Appl. Phys. **90**, 3750-3753 (2001).

[76] Y. Aoyagi, M. Takeuchi, S. Iwai, and H. Hirayama, "High hole carrier concentration realized by alternative co-doping technique in metal organic chemical vapor deposition", Appl. Phys. Lett. **99**, 112110 (2011).

[77] Á. Szabó, N. T. Son, E. Janzén, and A. Gali, "Group-II acceptors in wurtzite AlN: A screened hybrid density functional study", Appl. Phys. Lett. **96**, 192110 (2010).

[78] K. Irmcher, I. Gamov, E. Nowak, G. Gärtner, F. Zimmermann, F. C. Beyer, E. Richter, M. Weyers, and G. Tränkle, "Tri-carbon defects in carbon-doped GaN", Appl. Phys. Lett. **113**, 262101 (2018).

[79] I. Gamov, E. Richter, M. Weyers, G. Gärtner, and K. Irmcher, "Carbon doping of GaN: Proof of the formation of electrically active tri-carbon defects", J. Appl. Phys. **127**, 205701 (2020).

[80] I. Gamov, J. L. Lyons, G. Gärtner, K. Irmscher, E. Richter, M. Weyers, M. R. Wagner, and M. Bickermann, "Fingerprints of carbon defects in vibrational spectra of GaN considering the isotope effect", Phys. Rev. B. **106**, 184110 (2022).

[81] M. Steger et all., "Photoluminescence of deep defects involving transition metals in Si: New insights from highly enriched ^{28}Si", J. Appl. Phys. **110**, 081301 (2011).

[82] R. Jakiela, K. Sierakowski, T. Sochacki, M. Iwinska, M. Fijalkowski, A. Barcz, and M. Bockowski, "Investigation of diffusion mechanism of beryllium in GaN", Physica B: Phys. Condens. Matter 594, 412316 (2020).

[83] R. Czernecki, E. Grzanka, R. Jakiela, S. Grzanka, C. Skierbiszewski, H. Turski, P. Perlin, T. Suski, K. Donimirski, and M. Leszczynski, "Hydrogen diffusion in GaN:Mg and GaN:Si", J. Alloys and Compounds **747**, 354-358 (2018).

[84] S. Limpijumnong and C. G. Van de Walle, "Stability, diffusivity, and vibrational properties of monoatomic and molecular hydrogen in wurtzite GaN", Phys. Rev. B **68**, 235203 (2003).

[85] J.-S. Park and K. J. Chang, "Diffusion and stability of hydrogen in Mg-doped GaN: A density functional study", Appl. Phys. Express **5**, 065601 (2012).